Strike-slip faulting in the core of the Central Range of west New Guinea: Ertsberg Mining District, Indonesia

Benyamin Sapiie†
Mark Cloos‡
Department of Geological Sciences, University of Texas, Austin, Texas 78712, USA

ABSTRACT

Most of the Cenozoic tectonic evolution of the New Guinea region is the result of obliquely convergent motion that led to an arc-continent collision between the Pacific and Australian plates. Detailed structural mapping was conducted along road exposures in the Ertsberg (Gunung Bijih) Mining District in the core of the Central Range in the western half of the island. Two distinct stages of deformation are recognized. The first stage took place between ca. 12 and ca. 4 Ma and generated kilometer-scale folds with subsidiary reverse/thrust faults and strike-slip tear faults. Regionally, this deformation records many tens of kilometers of shortening. The second stage began at ca. 4 Ma and generated five northwest-trending (~300°) strike-slip fault zones up to a few tens of meters wide that are highly brecciated and contain numerous, mostly subparallel, planar faults. Each of these zones was a site of tens to a few hundred meters of left-lateral offset. Between these zones are domains containing three groups of planar strike-slip faults with orientations that are interpreted in terms of Riedel shears. (1) 040°–070° trending faults with left-lateral offset that plunge to the northeast (R shears), (2) 355°–015° trending faults with right-lateral offset that plunge to the N (R′-shears), and (3) 280°–300° trending faults with left-lateral offset that plunge to the northwest (D-shears). Subsidiary dip-slip faults (rakes > 45°) are associated with each group. Deformation in the district since ca. 4 Ma is best characterized as a left-lateral strike-slip fault system along an ~300° azimuth.

The change from tens of kilometers of shortening deformation that caused large-scale folding to a few kilometers of left-lateral strike-slip faulting occurred during the latest stage of collisional orogenesis. Although strike-slip faulting was a minor late-stage process, it was of profound importance in generating pathways for magma ascent and permeability for the rise of mineralizing fluids. The Grasberg Igneous Complex, the host of a supergiant Cu-Au porphyry copper–type ore deposit, was emplaced into a 2-km-wide, left-stepping pull-apart.

Keywords: New Guinea, Central Range, strike-slip, porphyry copper.

INTRODUCTION

The Ertsberg (Gunung Bijih) Mining District is located in the core of the Central Range of west New Guinea, next to Puncak Jaya (4884 m), the highest peak between the Himalayas and the Andes (Fig. 1). The origin of the island by continental drift was first discussed by Wegener (1929), and it was considered a type locality for arc-continent collision in the classic paper by Dewey and Bird (1970). Most of the Cenozoic tectonic evolution of New Guinea is the result of oblique convergence between the Australian and Pacific plates (Hamilton, 1979; Dow et al., 1988). The Central Range is commonly described as a fold-and-thrust belt, as spectacular folding is evident on aerial photographs and satellite images (Fig. 2). No outcrop-scale structural analysis had been done in west New Guinea until this investigation, which was made possible by the construction of mining roads.

One part of unraveling the tectonic evolution of the western Central Range involves understanding the relationships between deformation, intrusion, and mineralization. Two major questions are addressed: (1) What are the types, patterns, and distributions of outcrop-scale structures? (2) What is the relationship between deformation and the emplacement of intrusive rocks, particularly the Grasberg Igneous Complex—the host of a supergiant Cu-Au porphyry copper–type ore deposit. The data presented in this paper come from detailed analysis of structures exposed along the 10-km-long Heavy Equipment Access Trail (HEAT; called the HEAT Road herein) and the 5-km-long Grasberg mining access road (called the Grasberg Road herein; Fig. 2). Much of the faulting is very recent because in many places faults crosscut Pliocene intrusions.

REGIONAL GEOLOGY

The outline of the island of New Guinea has been described as similar to a bird flying westward with open mouth (Fig. 1). As a result, the island has been geographically divided into the Bird's Head, Neck, Body, and Tail regions. The central and largest part of the island (the Bird's Body) can be divided into four lithotectonic provinces: the New Guinea foreland, the Central Range fold-and-thrust belt, and a metamorphic belt with an overlying ophiolite complex that is the forearc basement of the accreted Melanesian island arc.

The New Guinea foreland (Arafura platform) is a swampy region of marine and nonmarine Pliocene and Holocene siliciclastic sedimentary rocks that are underlain by Cenozoic carbonate and Mesozoic siliciclastic strata deposited on the northern passive margin of Australia (Dow and Sukamto, 1984a, 1984b; Pigram and Panggabean, 1984). The Central Range orogenic belt stretches 1300 km from the Bird's Neck to the Bird's Tail. The 150-km-wide belt has rugged topography and numerous peaks over 3000 m in elevation. The Ruffaer metamorphic belt is a 1000-km-long and 50-km-wide zone of deformed, low-

†Present address: Departemen Teknik Geologi, Fakultas Teknologi Mineral, Institut Teknologi Bandung, Jl. Ganesha No. 10, Bandung 40132, Indonesia.
‡E-mail: cloos@mail.utexas.edu.

GSA Bulletin; March/April 2004; v. 116; no. 3/4; p. 277–293; doi: 10.1130/B25319.1; 17 figures.

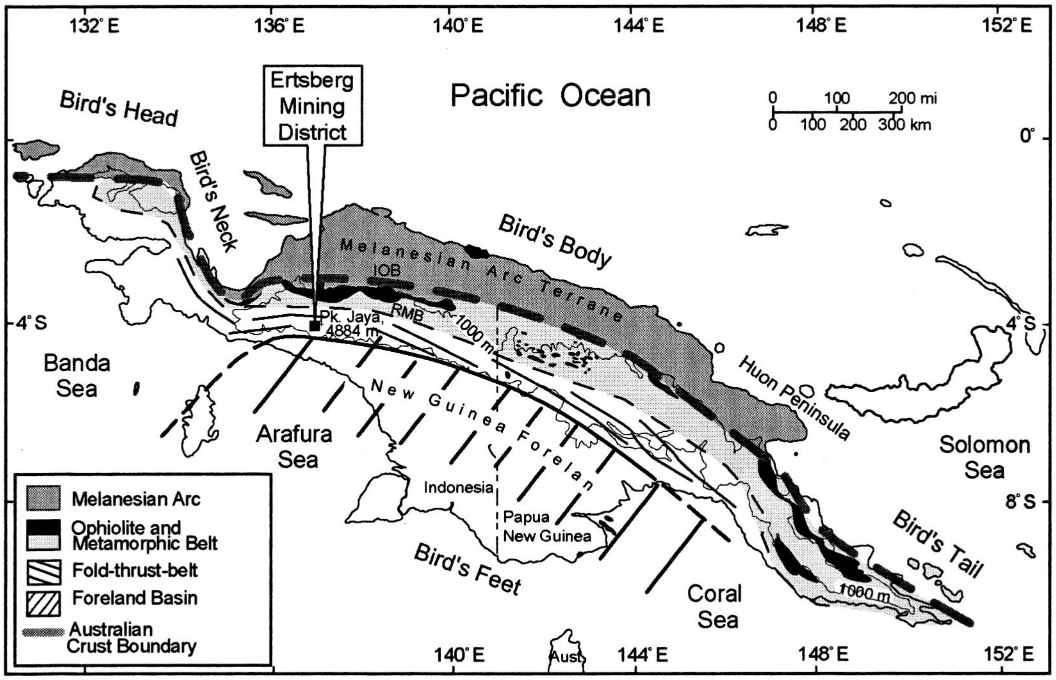

Figure 1. Lithotectonic map of the island of New Guinea. The Ertsberg (Gunung Bijih) Mining District is located within the P.T. Freeport Indonesia Contract-of-Work. RMB—Ruffaer metamorphic belt; IOB—Irian ophiolite belt; GIC—Grasberg Igneous Complex; GRS Rd.—Grasberg Road; HEAT Rd.—Heavy Equipment Access Trail Road.

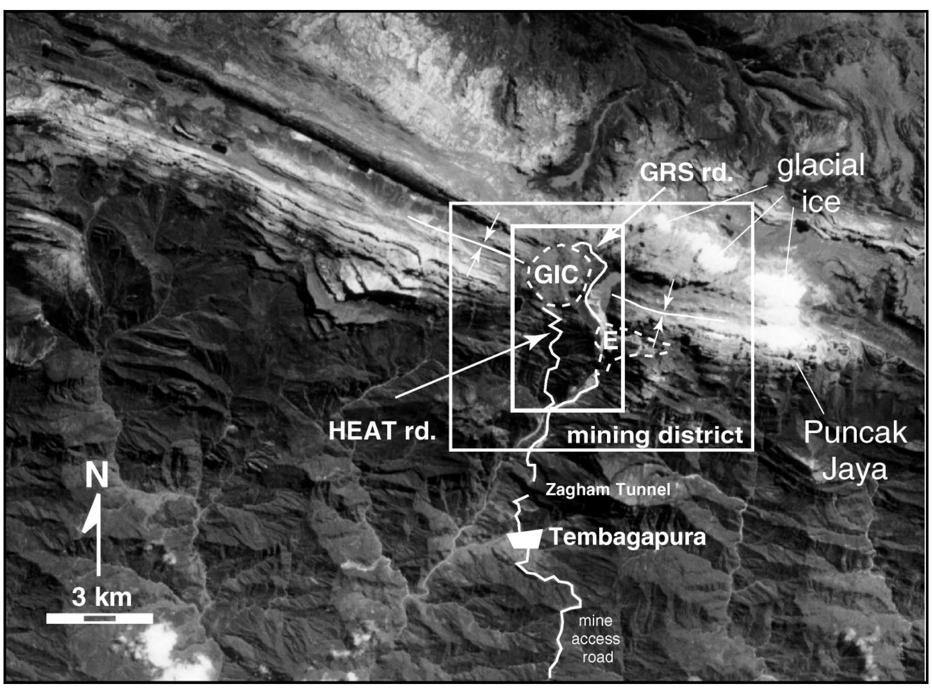

Figure 2. Satellite imagery (SPOT panchromatic image acquired in 1987) of the mining district, showing the location of the Ertsberg Mining District and the study area (inner solid box). GIC—Grasberg Igneous Complex, E—Ertsberg intrusion, HEAT rd.—Heavy Equipment Access Trail Road, GRS Rd.—Grasberg Road (both are merely for mine access).

temperature (<300 °C) metamorphic rocks that are bounded on the north by the Irian ophiolite belt and on the south by deformed, but unmetamorphosed, passive-margin strata (Dow et al., 1988; Granath and Argakoesoemah, 1989; Nash et al., 1993; Warren, 1995; Weiland, 1999). The Melanesian island-arc complex, built into the edge of the Pacific plate, is poorly exposed.

The details of the Cenozoic tectonic evolution in New Guinea are the subject of debate, as several kinematic models have been proposed. The most commonly published scenario is the subduction polarity reversal (''arc reversal'') model that entails movement of the Australian continental crust into a northward-dipping subduction zone, followed by collisional tectonism and initiation of southward subduction of the Pacific plate at the New Guinea Trench (Dewey and Bird, 1970; Hamilton, 1979; Milsom, 1985; Dow et al., 1988). An alternative model proposed to explain relationships in eastern New Guinea postulates that the island is underlain by a doubly subducted slab of oceanic lithosphere (''zippering'' model), which would be the westward continuation of the Solomon Sea plate (Ripper and McCue, 1983; Cooper and Taylor, 1987). Johnson et al. (1978) proposed a third model that is similar to the one involving northward-dipping subduction of the Australian plate, but in their model, subduction reversal has not oc-

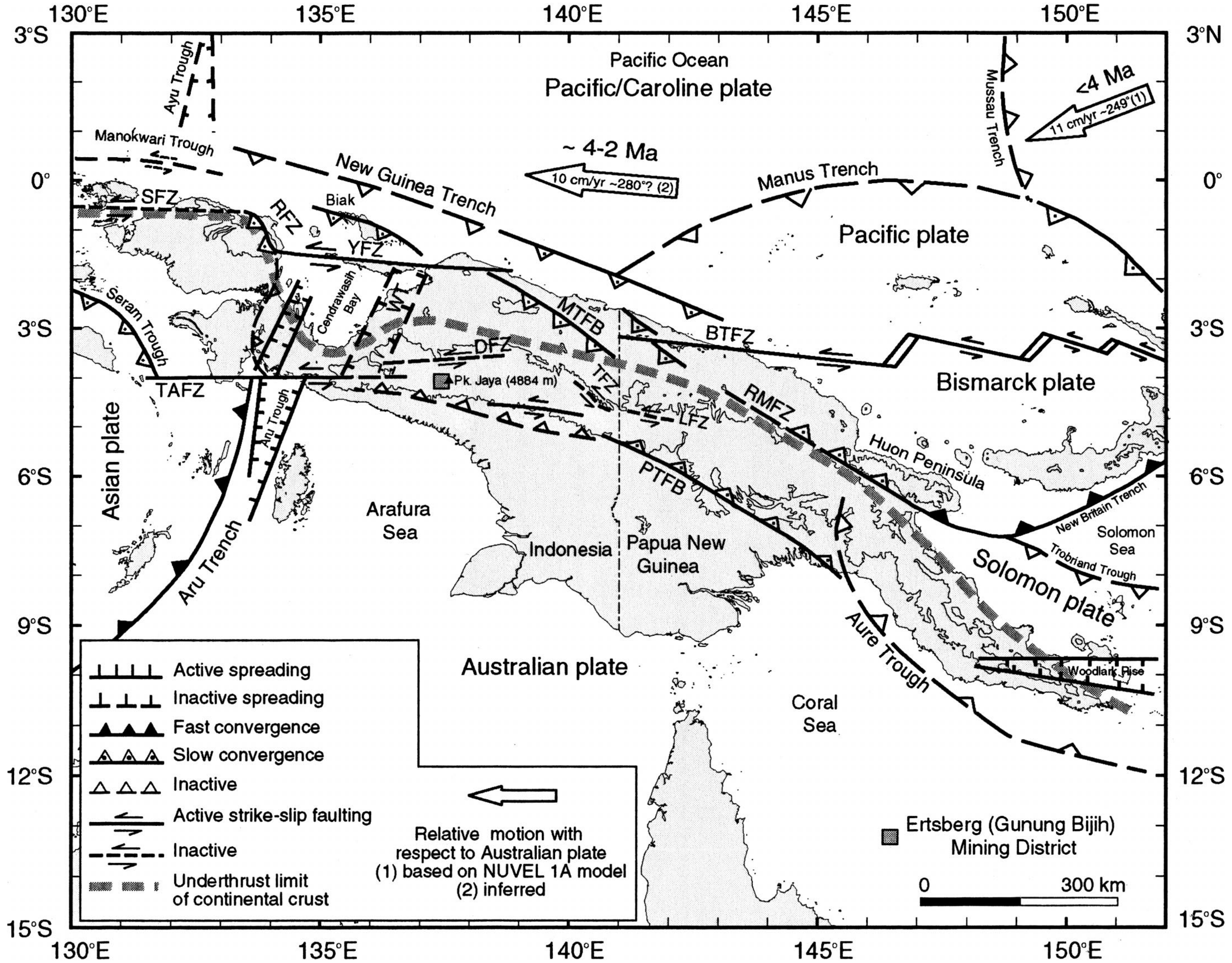

Figure 3. Seismotectonic interpretation of New Guinea. Tectonic features: PTFB—Papuan thrust-and-fold belt; RMFZ—Ramu-Markham fault zone; BTFZ—Bewani-Torricelli fault zone; MTFB—Mamberamo thrust-and-fold belt; SFZ—Sorong fault zone; YFZ—Yapen fault zone; RFZ—Ransiki fault zone; TAFZ—Tarera-Aiduna fault zone; WT—Waipona Trough. After Sapiie et al. (1999).

curred. In this scenario, the northward-subducted Australian lithosphere is thought to be dipping vertically.

The accumulating record of seismicity of the region does not delineate the southward subduction of the Pacific plate as envisioned by most workers. Abers and McCaffrey (1988) analyzed the focal mechanisms of the 18 largest earthquakes from 1964 to 1985 and found that more than half were roughly east-trending strike-slip movements, including six of the eight largest events near the Central Range. Sapiie et al. (1999) presented an analysis of the distribution of moderate and larger earthquakes ($M > 4$) from 1987 to 1997. Seismic activity is concentrated along the northern part of the island and near the eastern and western ends of the Central Range. In west New Guinea, there are few events deeper than 50 km, and there is remarkably little seismicity beneath where the Central Range elevations are higher than 1000 m. The overall seismicity indicates that most of the motion between the Australian and Pacific plates is accommodated by left-lateral slip along the Yapen and Bewani-Torricelli fault zones, which are connected by a wide convergent bend beneath the Mamberamo region near the international border (Fig. 3; see also Puntodewo et al., 1994). The Cendrawasih Bay area is a wide extensional bend bounded to the south where left-lateral slip occurs along the Tarera-Aiduna fault zone in the Bird's Neck region.

GEOLOGY OF THE ERTSBERG MINING DISTRICT

Stratigraphy

The stratigraphic units exposed in the mining district are part of the Jurassic–Cretaceous Kembelangan Group and the Tertiary New Guinea Limestone Group (Fig. 4). On the basis of regional lithostratigraphy, the contact between the Kembelangan and New Guinea Limestone Groups is conformable and located along the HEAT Road. Almost all of the sedimentary units along the HEAT Road dip steeply (~70°) to the north. With the exception of the stratigraphic duplication across the Wanagon fault and a minor fold, they show a

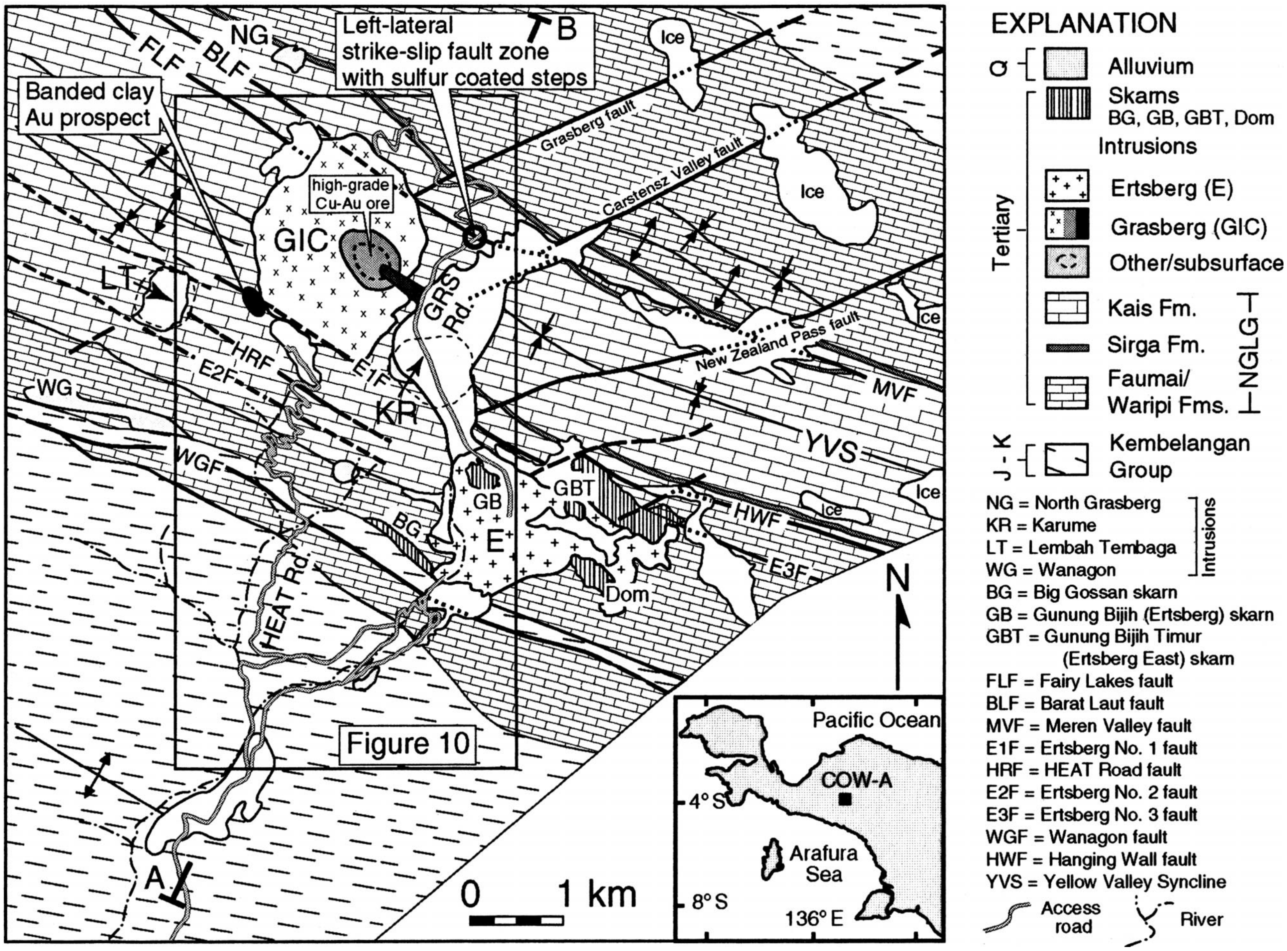

Figure 4. Geologic map of the Ertsberg Mining District, showing location of study area (box) and the HEAT and Grasberg (GRS) Roads. Modified from PTFI (P.T. Freeport Indonesia) base maps of Hefton and Kavalieris (1997) and Pennington and Kavalieris (1997). A–B—cross-section line in Figure 5. E—Ertsberg intrusion; GIC—Grasberg Igneous Complex; NGLG—New Guinea Limestone Group.

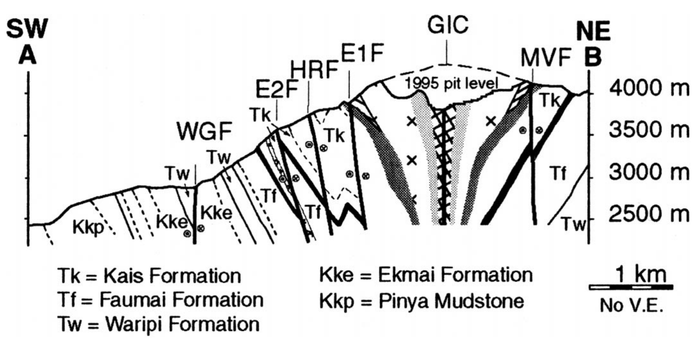

Figure 5. Cross-section A–B, showing relationship between major structures and sedimentary formations. Major fault zones have steep dips. Cross section is based on detailed field mapping at a scale of 1:5000. See Figure 4 for location, lithologies, and abbreviations.

simple homoclinal stratigraphic relationship in which the younger units crop out at the top of the mountain (Fig. 5A).

The Kembelangan Group is regionally extensive: it crops out in the Bird's Head and Central Range, and it is found in wells far south in the Arafura platform (Visser and Hermes, 1962; Pieters et al., 1983). In the mining district, this group consists of (1) interlayered carbonaceous siltstone and mudstone in the lower section and (2) fine-grained glauconitic quartz sandstone with minor shale in the upper section. At outcrop locations along the access road to the mining district, gray limestone is intercalated with clastic rocks (Martodjojo et al., 1975). On the basis of lithostratigraphic correlation with the regional stratigraphy (Quarles van Ufford, 1996), the Kembelangan Group in the mining district is divisible into two formations: the Pinya Mudstone and the overlying Ekmai Sandstone. This group was deposited as part of the Mesozoic passive-margin sequence conformably overlying the Triassic–Jurassic rift deposits of the Tipuma Formation (Dow et al., 1988; Parris, 1994).

The New Guinea Limestone Group overlies the Kembelangan Group. All four formations in the group, as originally defined by Visser and Hermes (1962), are well exposed in the mining district (Quarles van Ufford, 1996). The basal unit is the Paleocene to Eocene Waripi Formation that is composed of 400 m of fossiliferous dolostone, quartz sandstone, and minor limestone. The 300-m-thick Eocene Faumai Formation conformably overlies the Waripi Formation and is composed of thick-bedded (up to 15 m) to massive foraminiferarich limestone, marly limestone, dolostone, and a few quartz-rich sandstone layers up to 5 m thick. The lower Oligocene Sirga Formation unconformably overlies the Faumai Formation and is composed of a foraminifera-bearing, coarse- to medium-grained quartz sandstone and siltstone. Along the Grasberg Road, the sandstone beds have tabular cross-bedding and are locally pebbly with graded bedding. The thickness of the Sirga Formation along the HEAT Road is ~40 m, but probably varies greatly across the region. The Oligocene to middle Miocene Kais Formation conformably overlies the Sirga Formation. This 1100–1300-m-thick formation is composed of foraminiferal limestone with interbedded marl, carbonaceous siltstone, and coal. Biostratigraphic analysis indicates that the carbonate-shelf strata accumulated until at least 15 Ma and probably as late as 12 Ma (Quarles van Ufford, 1996).

Igneous Rocks and Mineralization

Igneous rocks are widespread in the district as small (meters to tens of meters wide) dikes, plugs, and sills. The two largest igneous bodies are the Ertsberg intrusion and the Grasberg Igneous Complex (Fig. 4). K-Ar biotite ages of 13 samples from large and small intrusions indicate that magmatism in the district took place between 4.4 and 2.6 Ma (McDowell et al., 1996). Geochemical and isotopic studies reveal that intrusions in the district can be divided into two distinct groups: a ''high-K'' and a ''low-K'' suite (McMahon, 1994a, 1994b, 1994c). This chemical difference is thought to be due to different degrees of lower-crustal assimilation by originally K-rich parental magmas from the mantle (McMahon, 2000a, 2000b; Housh and McMahon, 2000).

Two distinct classes of economic mineralization occur in the district: gold-rich copper skarns and porphyry-copper–type ore deposits (van Nort et al., 1991). The district is named for the Ertsberg skarn deposit, but is now renowned for the supergiant porphyry copper and gold deposit in the core of the Grasberg Igneous Complex (MacDonald and Arnold, 1994). At least three major skarn ore deposits occur next to the Ertsberg intrusion: the original Gunung Bijih (or Ertsberg), Gunung Bijih Timur (or Ertsberg East), and Dom (Mertig et al., 1994). The Big Gossan deposit occurs west of the Ertsberg and south of the Grasberg intrusions (Meinert et al., 1997). Deep, entirely subsurface porphyry copper (Lembah Tembaga) and skarn (Kucing Liar) systems were subsequently discovered near the southern boundary of the Grasberg Igneous Complex (Widodo et al., 1999).

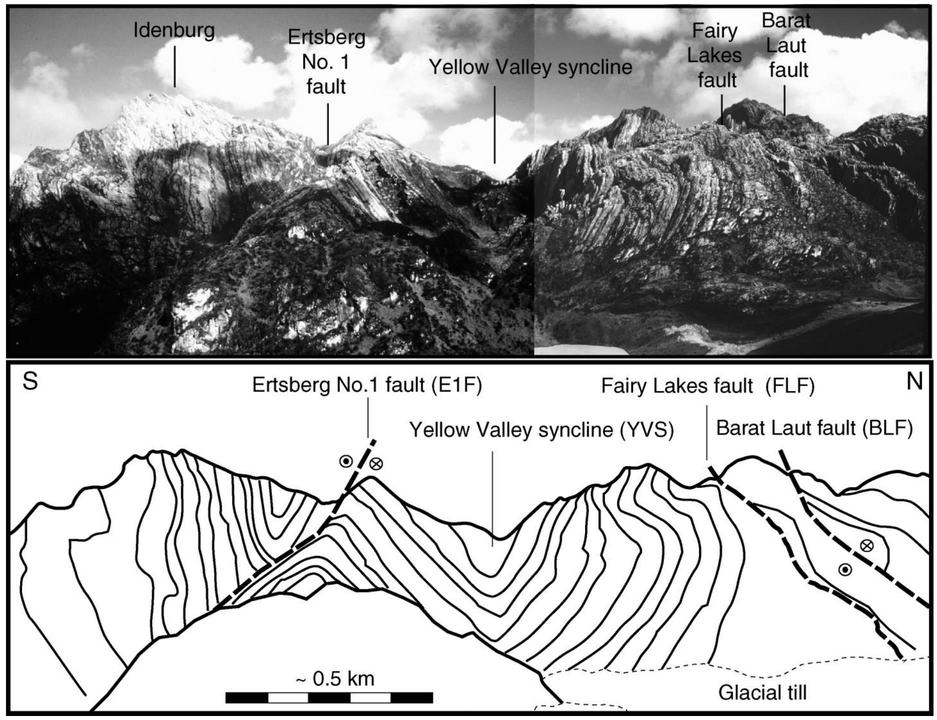

Figure 6. View looking to the west from the top of the Grasberg Igneous Complex, showing kilometer-scale folding of the New Guinea Limestone Group. The characteristic geometry is open symmetrical chevron folds with near-vertical axial planes. The Ertsberg No. 1, Fairy Lakes, and Barat Laut faults have near-vertical attitudes. Photomosaic by T.P. McMahon (photographs taken in 1992).

STRUCTURAL GEOLOGY OF THE MINING DISTRICT

The strata in the highlands underwent at least tens of kilometers of shortening deformation since 15 Ma. In the strata of the New Guinea Limestone Group, this deformation was accommodated primarily by kilometer-scale folding (Fig. 6). On the basis of fold patterns, shortening across the 10 km width of the mining district is 4 to 5 km (Quarles van Ufford, 1996). Shortening by faulting is much less obvious, and the field work for this paper was originally designed to estimate the nature and magnitude of such movements. It is evident that major shortening deformation in the mining district ended before ca. 4 Ma as the Grasberg Igneous Complex was emplaced as a plug that crosscuts the axis of the Yellow Valley syncline (Fig. 4).

This study involved detailed field mapping and structural analysis at a scale of 1:5000 (plate 1 in Sapiie, 1998). Structural data measured included the orientations of bedding, faults, slickensides (striations or grooves) or slickenfibers (mineral precipitates), and veins. Sense of shear on the fault planes was evaluated by using the criteria of Petit (1987). En echelon vein arrays and stylolites were also noted, but their occurrences were so rare and scattered that they did not provide significant kinematic information. The project was conducted during five field seasons and involved analysis of fresh outcrops that were created as the HEAT and Grasberg mine access roads were constructed. Because of steep topography, there was almost 90% rock exposure along these transects.

Kilometer-Scale Folding

Folding is so grand in character (Fig. 6) that many mine workers have assumed that understanding its origin was the key to understanding the controls on intrusion and mineralization in the district. Tertiary strata are deformed into chevron folds with open synclines and tight anticlines that are symmetrical and upright (interlimb angles of 40°–80°). The folds have a west-northwest trend with steeply dipping (>75°) to near-vertical axial planes (Fig. 4). Satellite imagery reveals that the kilometer-scale folds are arranged in an en echelon, left-stepping pattern that indicates a shortening direction of 210°–220° (Quarles van Ufford, 1996).

Calculation of a π-fold axis from the compilation of bedding measurements along the

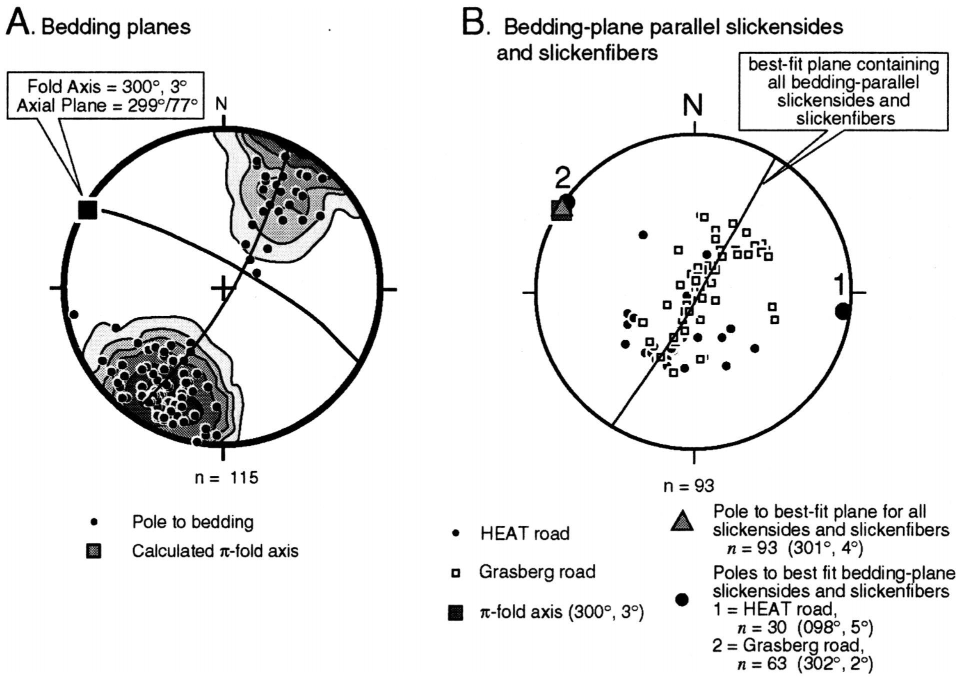

Figure 7. (A) Lower-hemisphere equal-area projection of poles to bedding and calculated π-fold axis for the New Guinea Limestone Group along the HEAT and Grasberg Roads. Axial-plane great circle was calculated by bisecting the bedding-plane population. (B) Orientation of slickensides and slickenfibers on bedding planes along the HEAT and Grasberg Roads.

Grasberg and HEAT Road yields a 300° trend and 3° plunge (Fig. 7). This result is comparable to a similar analysis by Quarles van Ufford (1996), who found that the average π-fold axis for the Cenozoic strata in the entire district has a 294° trend and 7° plunge.

Some bedding surfaces in the carbonate strata have slickensides and calcite slickenfibers. The π-fold axis and the pole to the calculated best-fit plane defined by these slip indicators are almost exactly parallel along the Grasberg Road but slightly discordant along the HEAT Road (Fig. 5B). Not surprisingly, these features indicate that flexural slip occurred on some bedding surfaces during folding. The orientation of these slips was obviously controlled by the anisotropy of the bedding, and they were therefore excluded from the analysis of the far more numerous faults that crosscut layering.

Faults

Faults in the study area are divided into ''major'' and ''minor'' groups. Major fault zones are preferentially eroded and thus form notches on ridges (Fig. 6). Linear grooves on mountainsides are traceable for several kilometers or more on satellite imagery and aerial photographs. Where roadcuts intersect the major faults, 2 to 50-m-wide zones of cataclastic breccia and/or clay gouge are found that contain numerous, planar faults (Fig. 8). These ''major'' faults are brittle shear zones along which repetitive episodes of slip occurred.

Minor faults are abundant within and between the brecciated fault zones. They are planar slip surfaces that extend to the limit of outcrop exposure, commonly several meters, but in some cases for several tens of meters. They are abundant north of the Wanagon fault zone. In the carbonate units, they almost always possess excellent kinematic indicators (Fig. 9). Nearly all of the more than 1300 minor fault planes measured along the HEAT and Grasberg Roads display only one orientation of slickensides. At only eight sites were two or more slip directions recognized on a fault plane. The conclusion is that nearly all of the minor faults are products of a single episodes of rupture with centimeters to tens of centimeters of slip in each movement.

Folding-Related Faults

Map relationships in the northeast corner of the mining district indicate the existence of three ~065°-trending faults that are related to folding (Fig. 4). The New Zealand Pass and Carstensz Valley faults are strike-slip tear structures that bound a 2-km-wide zone containing a minor syncline-anticline pair and a duplicated section of Sirga Formation. In this area, the Meren Valley fault is mapped as a reverse structure cutting obliquely between the duplicated section. Cross-section relationships indicate ~500 m of dip-slip offset (Quarles van Ufford, 1996).

A third tear fault, the Grasberg fault, is parallel to the other two. On the basis of the map pattern, this fault is a minor structure with only a few tens of meters of strike-slip offset. Between the Grasberg and Carstensz Valley tear fault, road construction revealed a fault zone that is on trend with the Meren Valley fault (Fig. 4). In the Grasberg roadcut exposures, there is clear evidence that the latest movements were left-lateral strike-slip, concurrent with some hydrothermal activity (discussed below).

Elsewhere in the mining district, only one other reverse fault is recognized at the surface from the inversion of stratigraphic order. The Wanagon fault crops out along the HEAT Road in the southern part of the district (Fig. 4). At this location, the Ekmai Formation is above the Waripi Formation, and there is at least 1000 m of apparent reverse offset (Fig. 5A). As found in the road exposure of the Meren Valley fault, the latest movements on the Wanagon fault were left-lateral strike-slip.

The Ertsberg #2 fault was first recognized where it was exposed during HEAT Road construction. At the road level, the Kais Formation is present on both sides, but exploration drilling reveals ~700 m of apparent reverse offset (Fig. 5A). The HEAT Road exposure shows that the latest displacement along this zone was also one of left-lateral strike-slip.

The Wanagon, Ertsberg No. 2, and the Meren Valley (at least in the northeast part of the district) faults have apparent reverse offsets of ~1000 m, 700 m, and 500 m, respectively. It has been stated and will be shown that the latest movements on each of these structures was left-lateral, strike-slip offset. Strike-slip movement oblique to steeply dipping bedding can, of course, create apparent dip-slip offset. This type of movement cannot account for the structural relationships near the Meren Valley fault in the northeast part of the district, but such movement could be responsible for the apparent dip-slip offset along the Wanagon and Ertsberg No. 2 faults.

Unfortunately, rigorous quantification of the amount of strike-slip offset that would cause the apparent dip-slip displacement is not possible because there are no piercing points and bedding dips in the folded terrane are variable with elevation. It is evident that several kilometers of left-lateral strike-slip offset would be required to account for apparent dip-slip along the Wanagon fault and somewhat less along the Ertsberg No. 2 fault. Such displacement must be have been concurrent with some sort of deformation to the southeast. The Ertsberg intrusion and related ore skarns are located where pull-apart dilation is inferred (discussed later). Although strike-slip offset alone does not appear to be adequate to account for the apparent dip-slip offset along these fault zones, it cannot be ruled out as the sole cause.

Nearly all bedding-plane slips measured along the HEAT and Grasberg Roads are parallel to those expected during flexural-slip folding (Fig. 5B). As dip-slip faulting was concurrent with the folding along the Meren Valley fault in the northeast part of the mining district, it seems most probable to us that the Ertsberg No. 1 and Wanagon faults also had an early history of high-angle reverse offset associated with the kilometer-scale folding. The origin of these fault zones is explained as being due to the folding's becoming sufficiently tight that continued shortening became accommodated, in part or entirely, by thrust or high-angle reverse faulting (see Twiss and Moores, 1992, p. 103).

On the basis of cross-section analysis and this discussion, shortening across the 10 km width of the mining district is 4 to 5 km by folding and up to 2 km by reverse faulting. It is thought that reverse faulting formed zones of weakness that were then reactivated as ''major'' strike-slip faults. The details of the postfolding strike-slip faulting is the focus of most of the rest of this report.

Postfolding Strike-Slip Faulting

Five left-lateral strike-slip fault zones were discovered subparallel to upturned bedding in exposures along the HEAT and Grasberg Roads (Fig. 10). Although there is little constraint on the amount of lateral displacement, the fault zones are considered ''major'' because the thickness of their breccia and numerous constituent planar faults indicate that they were sites of repeated offset. It is thought that each of these zones was a site of at least tens of meters to perhaps a few hundred meters of left-lateral strike-slip offset. Cumulative left-lateral displacement on all five zones could be on the order of 1 km. If displacements were many kilometers, greater stratigraphic irregularities should be evident. As these fault zones are nearly parallel to the overall trend of folding, a profound kinematic change must have occurred late in the deformation history.

From south to north, the five major strike-slip fault zones are Wanagon fault, Ertsberg No. 2 fault, HEAT Road fault, Ertsberg No. 1 fault, and Meren Valley fault. As discussed, three of these zones are apparently reactivated reverse faults (Wanagon, Ertsberg No. 2, Meren Valley). Three of the zones have evidence that some movement occurred after igneous intrusion (Wanagon, Ertsberg No. 2, HEAT Road). Four of the zones have evidence that some movement occurred after fluid inflow and mineralization (Wanagon, Ertsberg No. 2, Ertsberg No. 1, Meren Valley). These relationships indicate that faulting, igneous activity, and hydrothermal fluid flow were coeval.

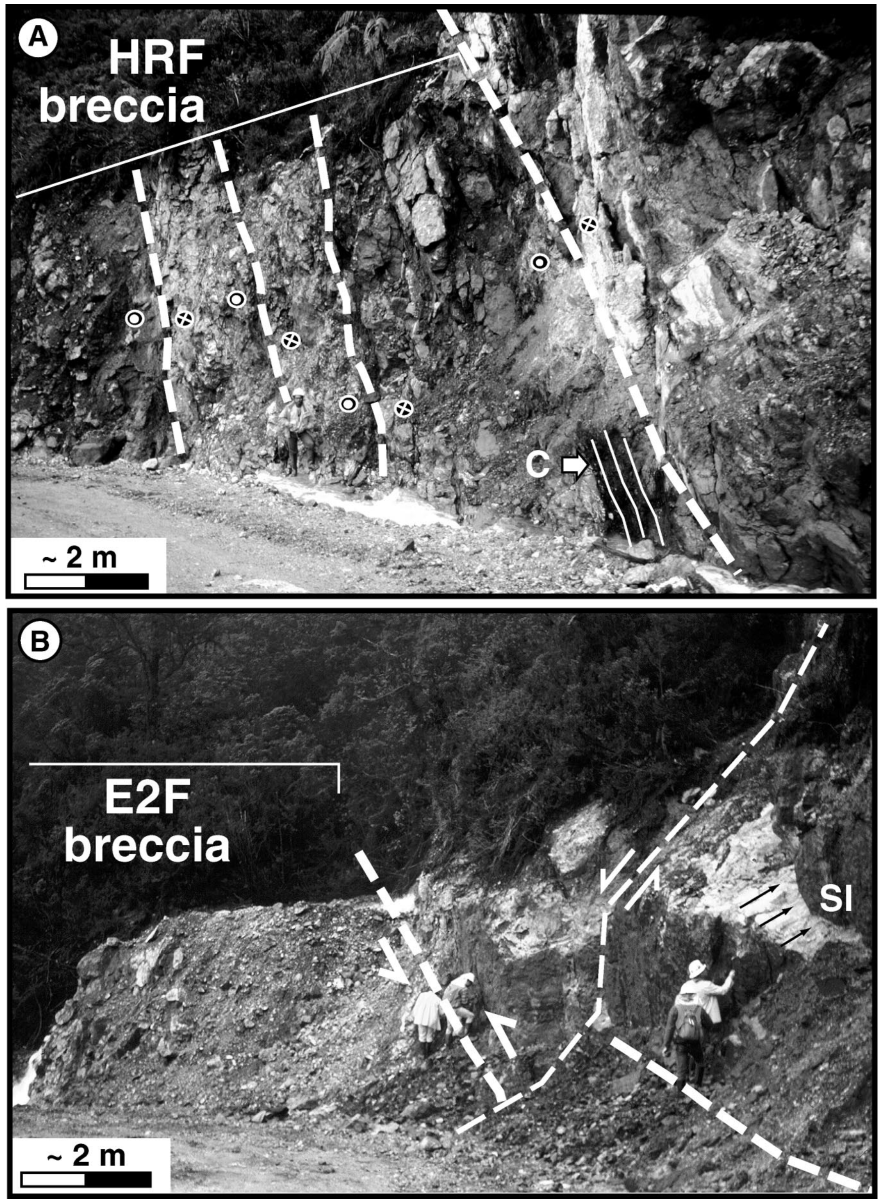

Figure 8. (A) HEAT Road fault (HRF) is a 15-m-wide zone. Four obvious fault planes are highlighted. Slickensides indicate left-lateral strike-slip movement. Location C is a localized site of solution cleavage in a clay-rich layer. (B) Ertsberg No. 2 (E2F) fault is a 10-m-wide cataclastic breccia zone. The boundary of this fault zone is crosscut by a northeast-trending left-lateral strike-slip fault with ~2 m of displacement. Near-horizontal, pyrite-coated slickensides are observed at location Sl (see Fig. 9B).

Wanagon Fault Zone

Along the HEAT Road, the Wanagon fault zone crops out at km 3.6 to km 3.8 (Fig. 10). An eroded groove can be traced west of the road for a distance of 2 km and east for more than 5 km. In the roadcut, a 50-m-wide zone of cataclastic breccia is composed of dolomite, dolomitic sandstone, and limestone from the Waripi Formation. Minor faults in this zone have an average trend of 302°/74°. The ma-

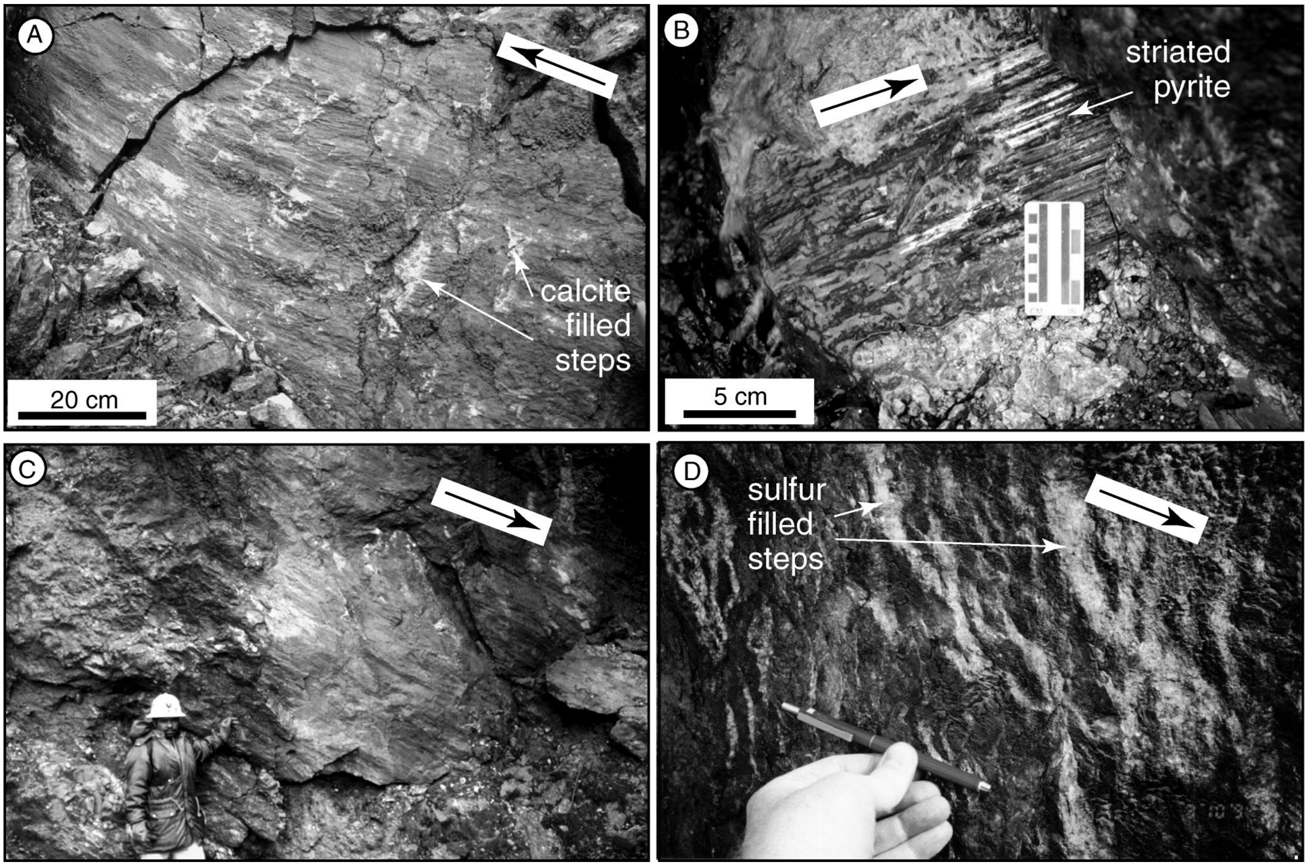

Figure 9. Examples of minor fault planes along the HEAT Road. (A) Near-vertical strike-slip fault with steps indicating right-lateral slip and slickenlines with an average rake of 15° (km 7.6). (B) Subhorizontal fault plane with pyrite slickensides in the Ertsberg No. 2 fault zone (km 6.8). (C) Vertical fault surface showing low-angle slickensides with a rake of ~20° and steps that indicate left-lateral offset (km 5.1). (D) Near-vertical fault plane within the Meren Valley fault-zone exposure along the Grasberg Road (see Fig. 4 for location), showing sulfur-filled steps and slickensides that indicate left-lateral strike-slip offset (arrow).

jority of slickensided surfaces indicate left-lateral displacement (Fig. 11). The Wanagon fault also contains brecciated dioritic dikes. Clasts and matrix contain disseminated and fracture-filling galena and sphalerite, indicating some movement after mineralization. Significant gold mineralization in the west Wanagon area may be related to this fault zone (S. Sukarya, 1993, personal commun.).

The excellent roadcut exposures of the Kembelangan Group along the HEAT Road also revealed that there are only a half dozen minor planar faults south of the Wanagon fault zone (Fig. 11). This zone must be a fundamental mechanical boundary in the district, for it marks the southern limit of abundant minor faulting. The significance of the spatial proximity of this fault to the southern boundary of the Ertsberg intrusion is discussed later.

Ertsberg No. 2 Fault Zone

Along the HEAT Road, the Ertsberg No. 2 fault zone crops out between km 6.6 and km 6.9 (Fig. 10). The corresponding groove in the hillside east of the HEAT Road intersects the road at km 6.3. An eroded depression in the mountainside can be traced west of the road for more than 2 km and to the east to near where it runs into the Ertsberg intrusion. In the roadcut, an ~10-m-wide zone of cataclastic breccia is composed of sandstone, siltstone, and limestone from the Kais Formation. Minor faults in this zone have an average trend of 297°/72°. The majority of the slickensided steps indicate left-lateral displacement (Fig. 11). At km 6.6, igneous dikes abut the Ertsberg No. 2 fault, and one dike containing veinlets of galena and sphalerite is brecciated.

The northern boundary of the Ertsberg No. 2 fault zone along the HEAT Road was offset several meters by a north-trending right-lateral strike-slip fault at km 6.6 (Figs. 8 and 10). The mapped eroded groove in the hillside east and west of the HEAT Road indicates that the fault zone was offset ~100 m in a right-lateral sense between km 6.3 and km 6.8.

HEAT Road Fault Zone

The HEAT Road fault zone crops out at km 7.8 on the HEAT Road (Fig. 10). An eroded depression in the mountainside extends over an ~2 km distance. To the west it trends into the Lembah Tembaga intrusion and to the east into the Ertsberg intrusion. In the roadcut, an ~30-m-wide zone of intensely cataclastic breccia and clay gouge is composed of carbonaceous siltstone, coal, and limestone of the Kais Formation. Most of the minor faults are found within black carbonaceous shales and thin coal layers, locally indicating strong lithologic control of movement. Minor faults in this zone have an average trend of 308°/76°. The majority of the slickensided steps indicate left-lateral displacement (Fig. 11). An igneous dike is present near this fault zone, but there is no indication of sulfide mineralization.

Ertsberg No. 1 Fault Zone

On the HEAT Road, the Ertsberg No. 1 fault zone crops out between km 9.3 and km

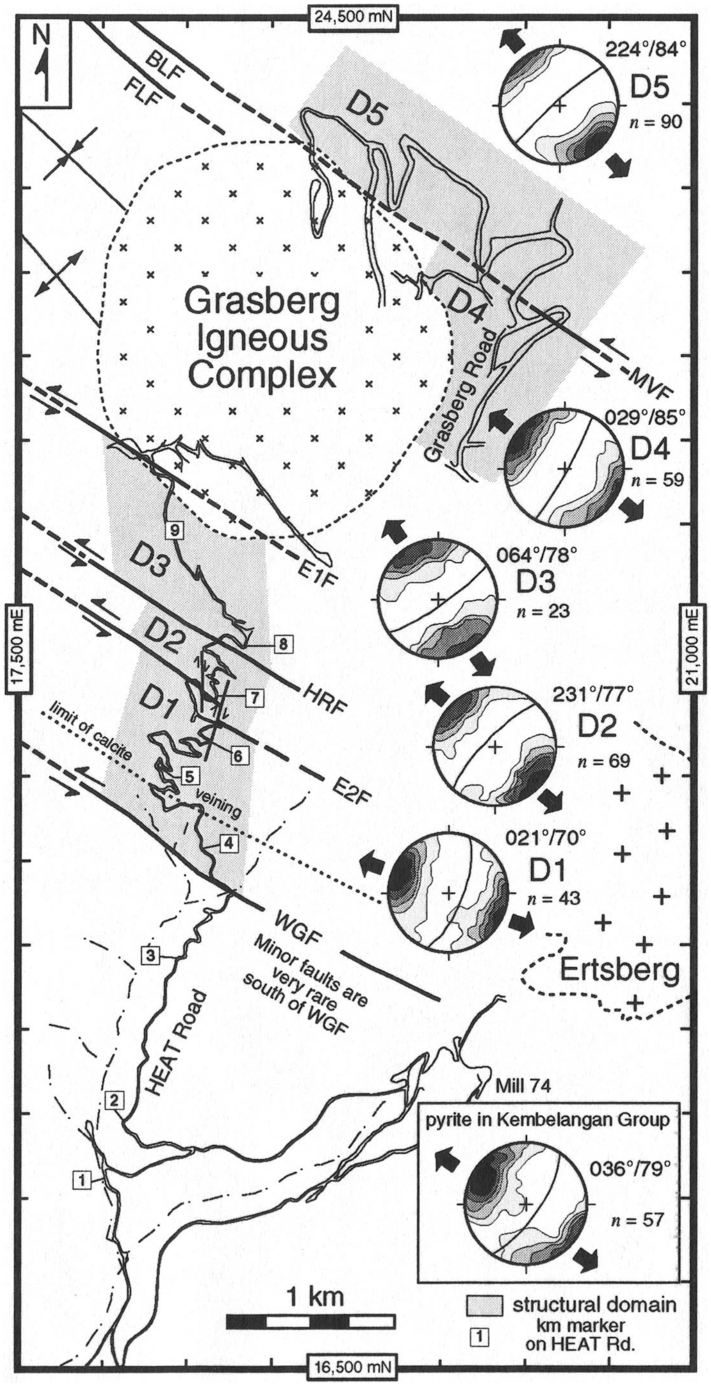

Figure 10. The HEAT and Grasberg Roads structural domains (D1, etc.). Stereonets show calcite-vein orientations in each domain. Pyrite veins are only abundant in the Kembelangan Group strata. Note the overall consistency in orientation. BLF—Barat Laut fault; MVF—Meren Valley fault; FLF—Fairy Lakes fault; E1F—Ertsberg No. 1 fault; HRF—HEAT Road fault; E2F—Ertsberg No. 2 fault; WGF—Wanagon fault.

9.5 (Fig. 10). An eroded depression in the mountainside is traceable westward for over an ~2 km distance where it passes the northern edge of the Lembah Tembaga intrusion. To the east it passes the northern edge of the Ertsberg intrusion, and it is nearly on line with the Hanging Wall fault zone that crosscuts the Gunung Bijih Timur skarn system. In the roadcut, an ~25-m-wide zone of cataclastic breccia and clay gouge is made of carbonaceous siltstone and limestone of the Kais Formation. Minor faults in this zone have an average trend of 294°/73°. The majority of the slickensided steps indicate left-lateral displacement (Fig. 11).

At the edge of the Grasberg Igneous Complex, the Ertsberg No. 1 fault intersects the "banded clay" unit that is the host of epithermal mineralization with gold contents as high as 10 ppm (Fig. 4; C. Brannon, 1991, personal commun.). The breccias along the southern side of the Grasberg Igneous Complex ("marginal breccia") and the Kucing Liar orebody, a deep zone of copper-skarn mineralization, are spatially associated with this fault zone.

Meren Valley Fault Zone

The westward continuation of the Meren Valley fault as mapped in the northeast part of the mining district intersects the mine access road ~1 km northeast of the center of the Grasberg ore zone (Fig. 4). As discussed, reverse offset of ~500 m is evident from field relationships in the northeast part of the district. Where this fault crops out along the Grasberg Road, it is between the Grasberg and Carstensz Valley tear faults. A minor, early history of perhaps tens of meters of reverse slip is probable. Minor faults are numerous with an average trend of 298°/81° (Fig. 11).

The Meren Valley fault is nearly on trend with the Barat Laut and Fairy Lakes faults in the northwest part of the mining district (Fig. 4). There is no evidence of an earlier history of dip-slip offset on these two faults. It is concluded that when the Meren Valley fault was reactivated as a left-lateral strike-slip fault in the eastern and central parts of the mining district, the Barat Laut and Fairy Lakes faults formed to accommodate some of this displacement in the northwestern part of the district.

The outcrop of the Meren Valley fault zone along the Grasberg Road is an ~2-m-wide breccia that is distinctly different from the others. First, clasts in the zone contain an asymmetric fabric and a pressure-solution cleavage. Second, numerous sulfur-filled veins and spectacular sulfur-coated slickensides and sulfur-filled steps record left-lateral strike-slip offset (Fig. 9D). The sulfur-coated slickensides and sulfur-filled steps indicate that strike-slip faulting along the Meren Valley fault was concurrent with magmatic degassing. The development of a cleavage probably resulted from higher temperatures in this area at the time of movement.

Minor Strike-Slip Faults

The roadcuts created for the HEAT and Grasberg Roads also revealed that the strata

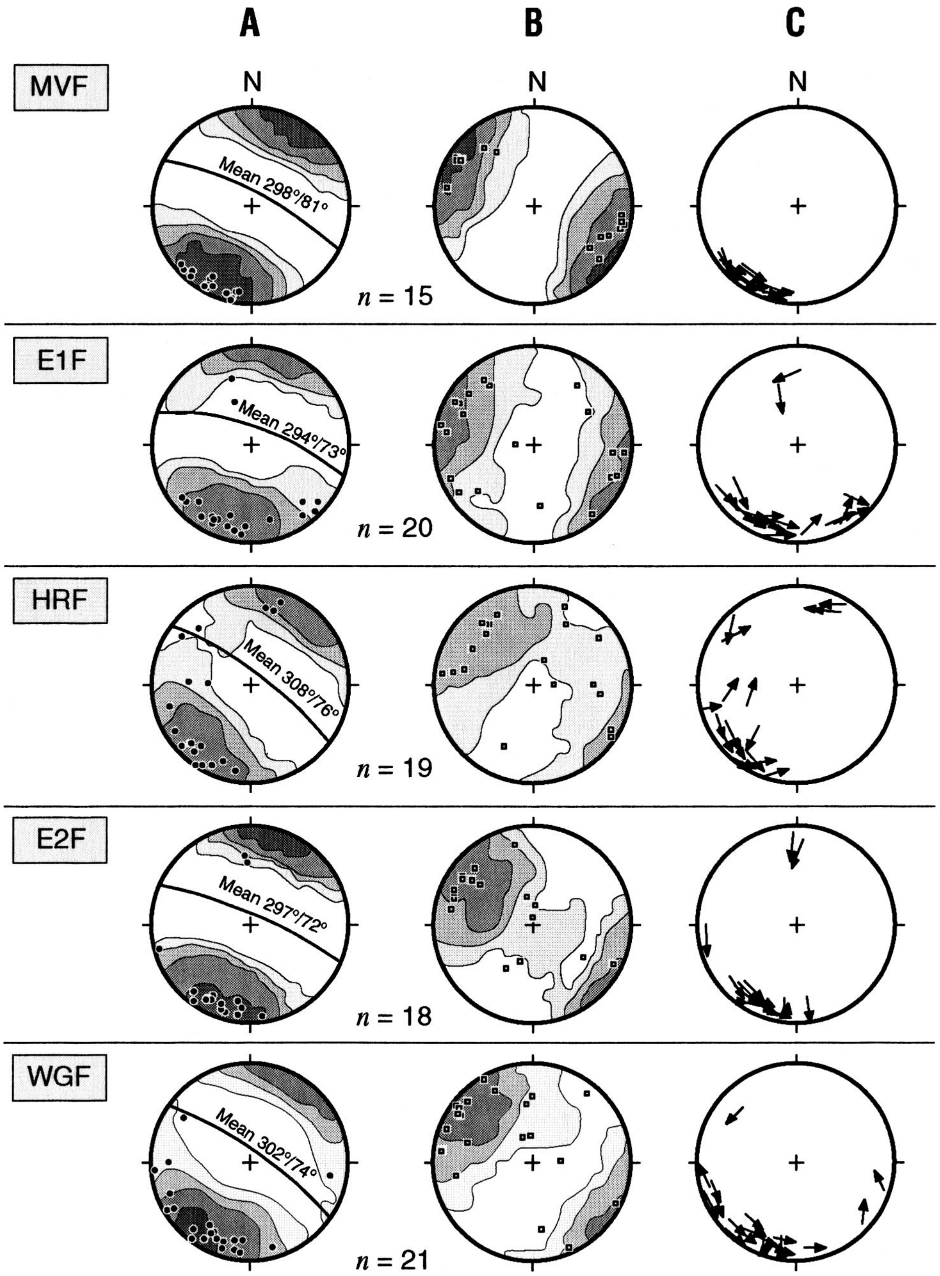

Figure 11. Lower-hemisphere equal-area stereograms show the distribution of fault planes within the major fault zones. (A) Poles to faults (filled circles) and contoured. (B) Slickensides (squares) and contoured. (C) Slip linear diagram represented by arrows showing direction of slip of the footwall block in which arrow is drawn parallel to movement direction along the fault. Kamb (1959) contour interval = 2σ. MVF—Meren Valley fault; E1F—Ertsberg No. 1 fault; HRF—HEAT Road fault; E2F—Ertsberg No. 2 fault; WGF—Wanagon fault.

north of the Wanagon fault zone (Fig. 11) are crosscut by numerous minor planar faults with a wide variation in orientation (Fig. 12). The most notable attribute of these data is that minor fault attitudes do not parallel the ~300° trend of the five major, mappable fault zones. Northeast trends are dominant. Along the Grasberg Road, most slickensides and slickenfibers indicate near-horizontal (plunges <15°) strike-slip offset. There is a northeast-trending girdle and secondary maxima with a plunge near 80°NE that are, at least in part, from the inclusion of minor planar faults that formed during flexural-slip folding. Along the HEAT Road, near-horizontal offsets are also dominant; distinct maxima have plunges of 15°, 25°, and 60° to the southwest (Fig. 12). Again, some of the steeper plunges are probably from movements during flexural-slip folding.

Steps along planar faults provide the evidence for sense of shear. Of 1392 fault planes measured, two-thirds exhibited very good to excellent kinematic indicators. In this paper, faults are divided into two types: strike-slip faults with rakes of <45° and dip-slip faults with rakes of >45°. The histogram of rake-angle distribution shows that ~70% of the fault-slip data fall into the category of strike-slip offset and that rakes of 5°–15° are abundant (Fig. 13A). The distribution of fault types based on kinematics can be evaluated by using the relationship of dip of fault vs. slip-vector rake (Fig. 13B). Overall, left-lateral offsets outnumber right-lateral offsets. Left-lateral offsets are dominant along the HEAT Road traverse, but right-lateral and left-lateral offsets are equally abundant along the Grasberg Road transect. The plot of dip of fault vs. slip-vector rake shows that most dip-slip faults have normal offset along the HEAT Road, but that both normal and reverse offsets are similarly abundant along the Grasberg Road (Fig. 13B). The plot of strike of fault vs. slip-vector rake reveals that right-lateral faults are dominated by 355°–010° trends and left-lateral faults are dominated by 050°–080° trends (Fig. 13C). Dip-slip faults show highly scattered distributions with weak clusters having 040°–090° trends.

These data indicate that the minor but numerous planar faults along the transects are dominantly along steeply dipping surfaces that record both left-lateral and right-lateral strike-slip offset. The overall character of minor movements appears to be somewhat different north and south of the Grasberg Igneous Complex, as left-lateral strike-slip movements outnumber right-lateral movements and dip-slip faults with normal offset are more abundant than ones with reverse offset along the HEAT Road.

Structural Domains

To evaluate the homogeneity of faulting between the major fault zones, the HEAT and Grasberg Road transects were divided into five structural domains (Fig. 10). Three domains (D1, D2, D3) are along the HEAT Road transect (Fig. 14), and two (D4 and D5) are along the Grasberg Road transect (Fig. 15). On the basis of kinematic indicators, the faults in the domains were divided into three types: left-lateral strike-slip faults, right-lateral strike-slip faults, and dip-slip faults (rake >45°).

The stereographic analysis of minor fault

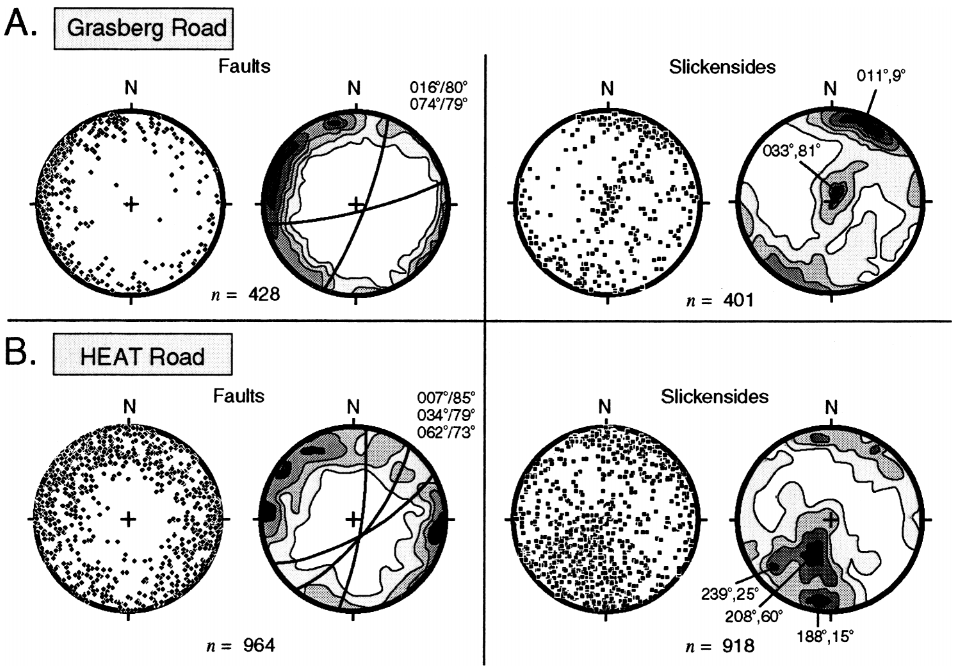

Figure 12. Lower-hemisphere equal-area projections of poles to faults (dots) and of trends and plunges of slickensides (squares) for all data from HEAT and Grasberg Roads. Kamb (1959) contour interval = 2σ. Great circles are representative fault planes for point maxima.

data shows remarkable similarity for all five domains. Right-lateral faults have a strong preferred trend of 355°–010°. Left-lateral faults have a strong preferred trend of 055°–080° with subsidiary 280°–300° trends in some domains. Dip-slip faults have two common trends: 020°–080° and 280°–310°. Along the HEAT Road, right-lateral strike-slip faults were more commonly observed to crosscut left-lateral faults. This was a mappable relationship for the northern boundary of the Ertsberg No. 2 fault zone along the HEAT Road.

Extension Fractures

Veins in the mining district are mineralized extension fractures. They are abundant along the HEAT and Grasberg Roads within the New Guinea Limestone Group. Most veins are calcite with local occurrence of minor quartz. Rarely, calcite veins were found with center lines of pyrite. Some have open spaces in the center. In the sandstone of the Ekmai Formation, pyrite-only veins are present. As with faulting, veining is very rare south of the Wanagon fault zone (Fig. 10).

Calcite veins are typically nearly vertical and ~1 mm wide, but a few are up to 50 mm wide. Most are isolated with a length-to-width ratio of 5:1 to 10:1, but some extend for several meters. Some are gently curved. En echelon sets were observed at five locations, and the kinematic information they provided matched that from nearby faults. Sigmoidal veins were not observed. Offset of matching vein-wall irregularities and host-rock structures clearly indicates a dilational origin. Most are at high angles (60°–90°) to local bedding orientation. Petrographic analysis indicates that calcite crystal growth occurred approximately normal to the vein walls, and no crack-seal textures were observed. Veins appear to be the product of a single opening and filling event.

Pyrite veins in the sandstone of the Ekmai Formation of the Kembelangan Group (Fig. 10) have thicknesses that vary from paper-thin to several millimeters. Most of these veins have simple tabular geometries, and some extend for several tens of meters. Commonly, they occur in parallel sets that crosscut bedding at high angles (70°–80°).

The direction of incremental extension is assumed to have been perpendicular, or nearly so, to the vein walls. Stereographic analysis of the veins was done in groupings based on the five structural domains defined by the major fault zones (Fig. 10). As with minor planar faulting, the mean orientations of veins are remarkably uniform in each domain. A strong preferred northeast trend indicates a consistent northwest-southeast direction of extension nearly parallel to the ~300° trends of the major fault zones. In domains D1, D2, and D3 along the HEAT Road, minor faults with normal offset are more common than ones with reverse offset (Fig. 13B). The normal fault trends are consistent with the northwest-southeast extension recorded by the veins, and this fact suggests that the normal faults and veins are coeval.

INTERPRETATION

Field studies in the core of the western Central Range revealed abundant evidence that a systematic pattern of faulting is superimposed on the kilometer-scale folds. Five major left-lateral strike-slip fault zones in the Ertsberg Mining District bound domains containing numerous, minor, right- and left-lateral strike-slip faults. Dip-slip faults are dominantly of normal type along the HEAT Road transect, but normal and reverse slip faults are similarly abundant along the Grasberg Road. Across the area, a northwest-southeast direction of extension is recorded by veins.

Riedel Shear System

The pattern of strike-slip faulting along the Grasberg and the HEAT Road traverses can be interpreted by comparison with the classic clay-cake experiments of Riedel (1929), which were refined by Tchalenko (1970). In these experiments, a layer of clay atop two boards is found to develop a systematic pattern of faults, ''Riedel shears,'' as one of the boards is slid past the other to simulate strike-slip offset in crystalline basement. During the initial stages of offset, two distinct sets of Riedel shears (R and R′, and D) develop in the clay cake. R and R′ shears are distinctly oblique to the ''basement fault,'' but D shears are subparallel. As offset continues, D shears form parallel to the underlying basement fault, and eventually a throughgoing fault zone develops in the clay layer that is directly above the basement fault. As this ''major faulting'' occurs, displacement on the minor Riedel shears ceases.

Minor faults within the major strike-slip fault zones have average trends of 302°, 297°, 308°, 294°, and 298°. These orientations average 299°, a trend that is nearly parallel to the ~300° trend of upturned bedding. The upturned bedding is a major anisotropy that obviously played a significant role in localizing the zones of fault movement. However, this alone cannot account for the activation of the late-stage left-lateral strike-slip fault system subparallel to the upturned bedding. Minor faults in the zones have average dips to the northeast that range from 72° to 81° (Fig. 11). Such dips are significantly greater than the lo-

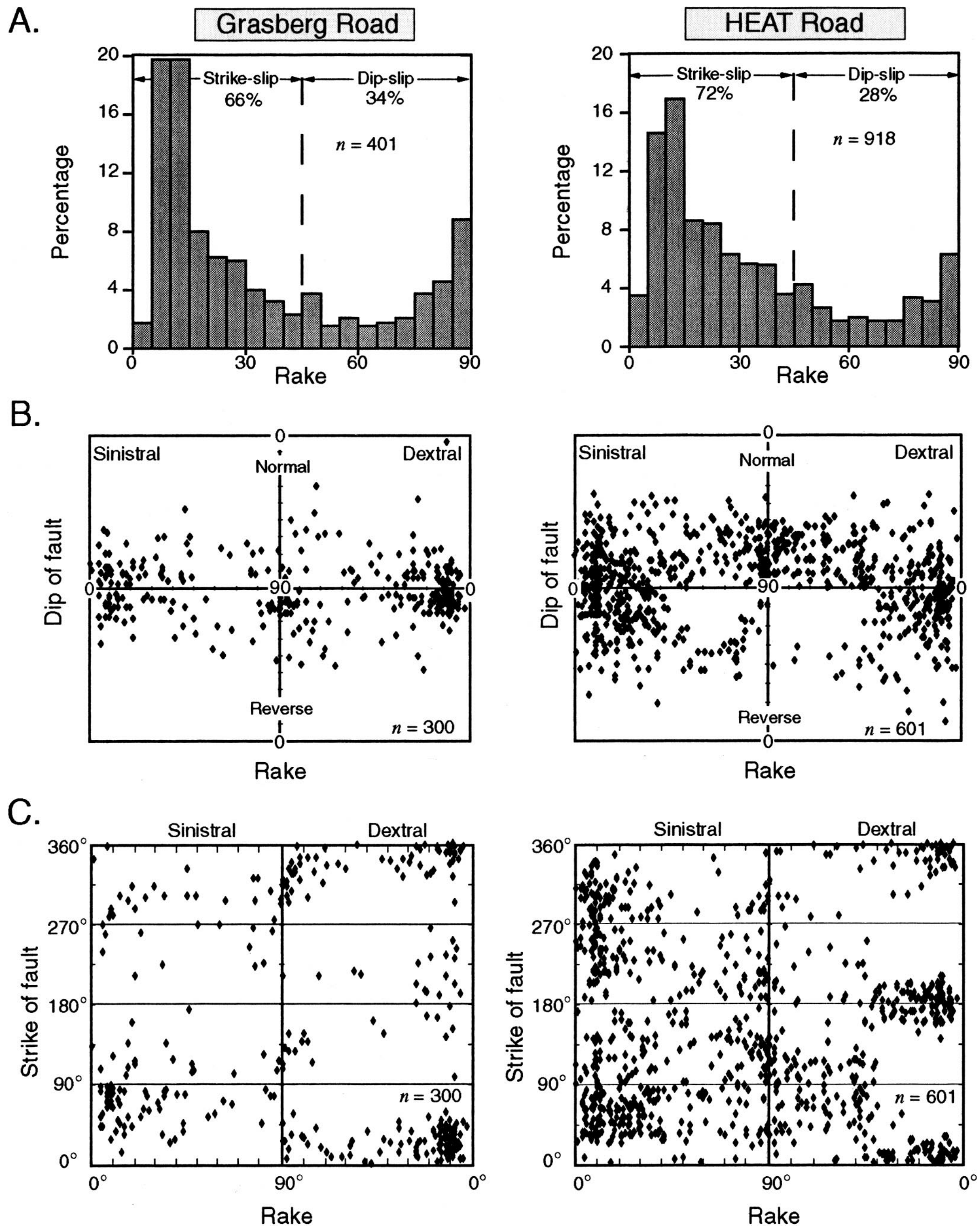

Figure 13. (A) Histogram of rakes for slip lineations measured along the Grasberg and HEAT Roads. A rake value of 45° is the cutoff between strike-slip and dip-slip faulting. (B) Dip of fault vs. slip-vector rake (adapted from Little, 1995) for faults along the Grasberg and HEAT Roads. Note the abundance of normal offset in the HEAT Road data compared to the Grasberg Road data. (C) Strike of fault vs. slip-vector rake for faults along the Grasberg and HEAT Roads.

cal bedding dip and even opposite in direction in the case of the Meren Valley fault (Fig. 5). As the major fault zones are steeply dipping and the bedding is of variable attitude, the mean fault zone trend of ~300° is interpreted as nearly parallel to left-lateral displacements rooted in the underlying crystalline basement. The nucleation of a left-lateral strike-slip fault system trending 300° would be most favored if the relative measurements were along basement anisotropies that trended ~300°. Similarly, the strike-slip activation of basement anisotropies trending northwest would induce such movements in the upturned sedimentary cover. Regional evidence for basement anisotropies with a trend of ~280°/100° and a regional kinematic change at ca. 4 Ma is discussed subsequently.

With the interpretation that the major left-lateral fault zones are subparallel to displacement zones in the basement and under the assumption that the local lithologies behaved as Coulomb materials, the orientation of Riedel shears is predictable (Tchalenko, 1970). R shears should form 40°–65° measured clockwise from the ~300° trend, which corresponds to left-lateral strike-slip faults trending ~055°–080°. R′ shears should form 90°–105° clockwise from the 300° trend, which would correspond to right-lateral strike-slip faults

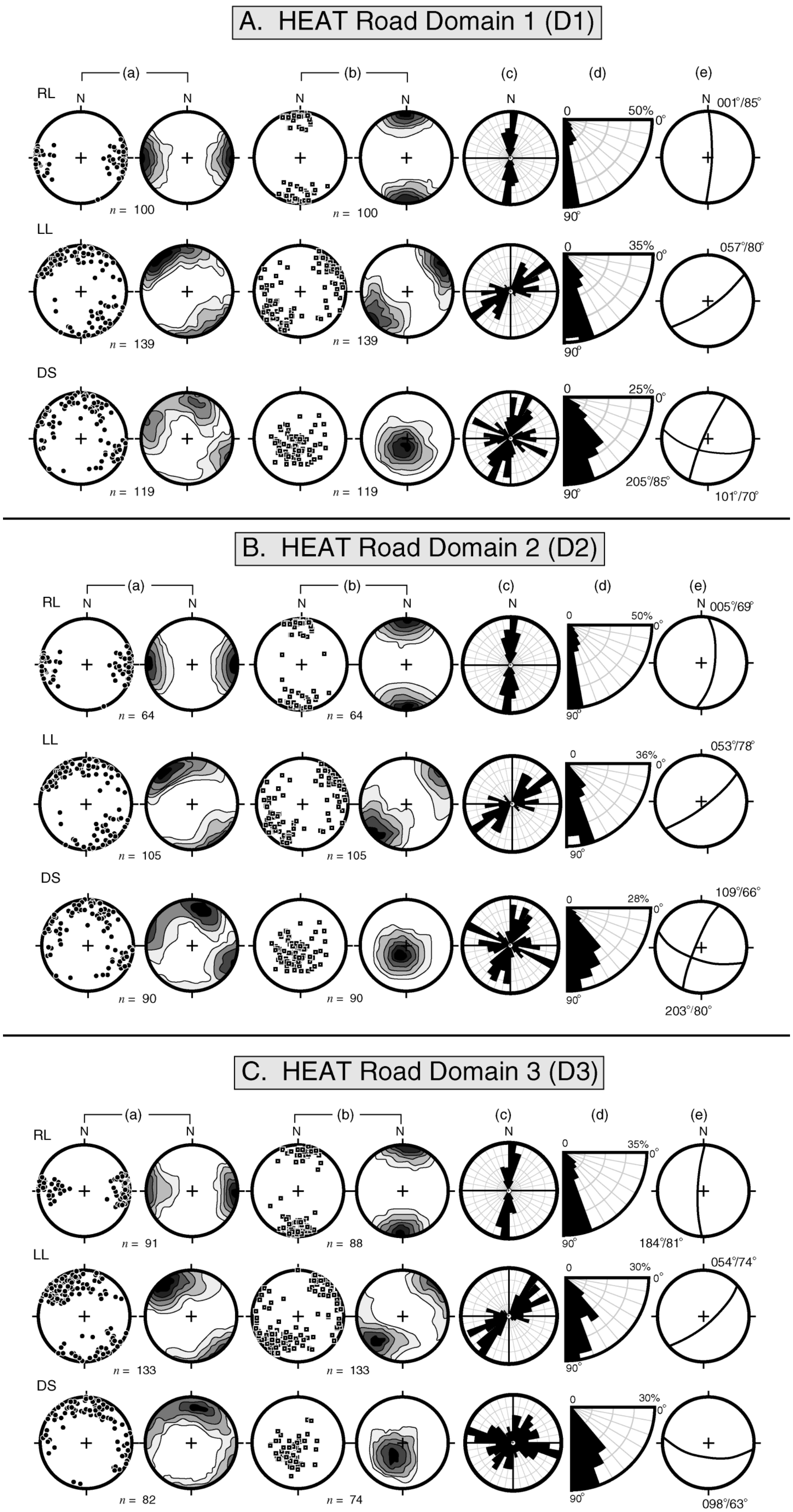

trending ~355°–015°. Left-lateral strike-slip faults trending 280°–310° are D shears.

The orientation and sense of offset along minor faults near the Grasberg Igneous Complex is in remarkable agreement with the orientation and sense of offset predicted by analogy with simple strike-slip clay-cake experiments (Fig. 16). Such agreement requires that rotations during progressive simple shear were small (<10°–20°), a condition readily attained if the cumulative left-lateral offset was 1 km or so at most.

Igneous Activity and Strike-Slip Faulting

In the mining district, igneous activity occurred between 4.4 and 2.6 Ma. The Grasberg and Ertsberg intrusions are host to economically major Cu-Au mineralization (Fig. 6). Thus, one of the most important questions concerns the emplacement of these plutons. Wall-rock xenoliths, changes in bedding attitudes of the wall rocks, and flow foliation, as described by Hutton (1982, 1990) for settings where intrusion was forceful, are notably scarce in the mining district. The igneous bodies in the mining district were passively emplaced, as is the case for most plutons hosting porphyry-copper–type deposits (Sillitoe, 1973; Titley, 1981).

The Ertsberg intrusion is a large equigranular intrusion with a volume of several tens of cubic kilometers. The bulk of this pluton appears to have been emplaced in one large pulse as a thick laccolithic sill that then slowly cooled (McMahon, 1994a, 1999). Copper mineralization is localized in the Gunung Bijih, Gunung Bijih Timur, and Dom skarn ore systems that have the form of tall, crudely cy-

Figure 14. Fault data from HEAT Road structural domains plotted in lower-hemisphere equal-area stereonet and rose diagrams. (A) Domain 1 (D1) between the Wanagon fault and the Ertsberg No. 2 fault. (B) Domain 2 (D2) between the Ertsberg No. 2 fault and the HEAT Road fault. (C) Domain 3 (D3) between the Ertsberg No. 1 fault and the HEAT Road fault. Domain boundaries are shown in Figure 10. Columns of plots: (a) Poles to faults (dots) and contoured diagrams. (b) Slickenside trend and plunge (squares) and contoured diagrams. (c) Rose diagram of fault trends. (d) Rose diagrams of fault dips. (e) Representative fault planes from point maxima in Kamb contour diagrams. RL—Right-lateral strike-slip faults, LL—Left-lateral strike-slip faults, DS—Dip-slip faults.

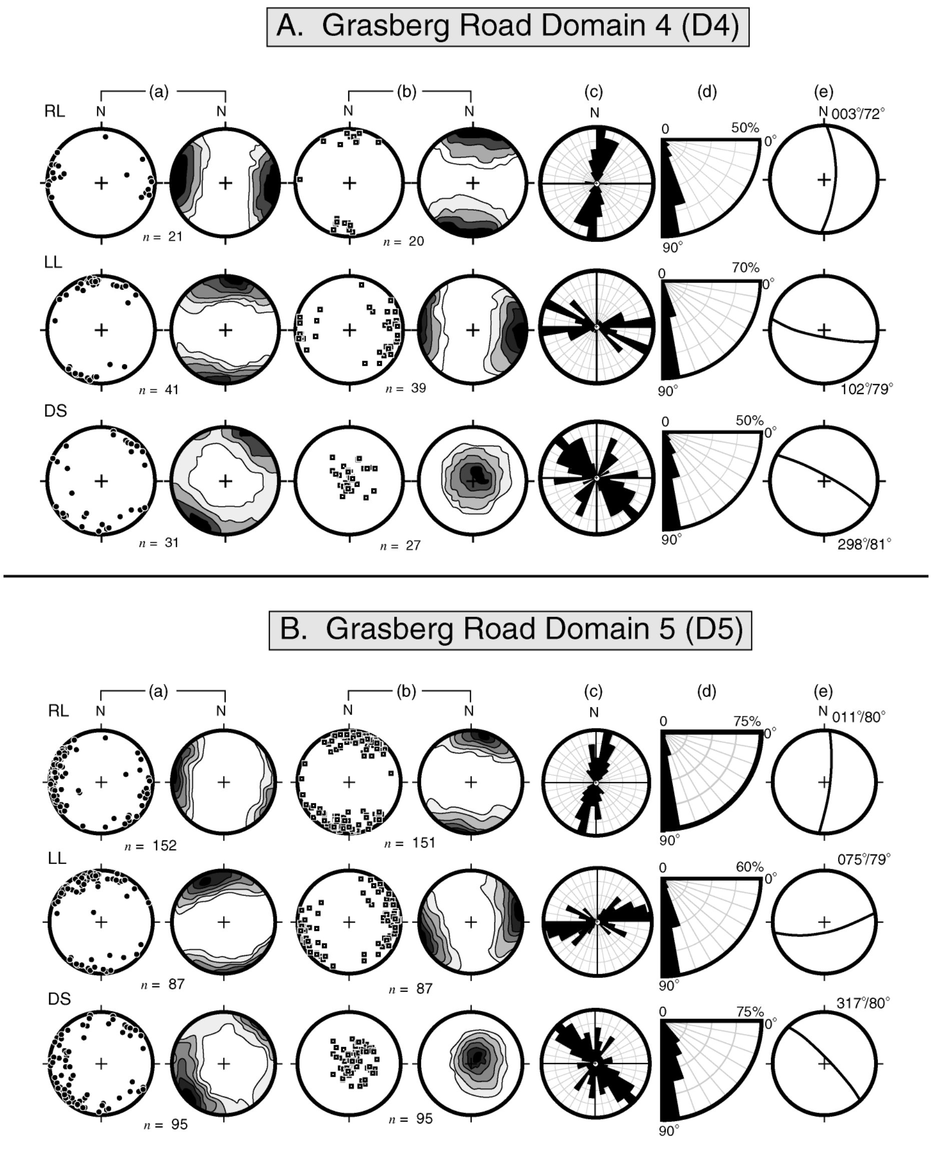

Figure 15. Grasberg Road structural domains. Lower-hemisphere equal-area stereonet and rose diagrams of fault data from (A) domain 4 (D4) south of the Meren Valley fault and (B) domain 5 (D5) north of the Meren Valley fault. For explanation and abbreviations, see Figure 14.

lindrical bodies. The Grasberg Igneous Complex has a more complicated three-stage magmatic history. Major copper-gold mineralization postdates the second stage, but predates the third.

Dilational domains along major strike-slip fault systems have been proposed as a simple solution to the problem of generating space for the emplacement of granitic plutons (e.g., Hutton, 1990; Glazner, 1991; Tikoff and Teyssier, 1992). Paterson and Fowler (1993) argued that complexes of dikes or sheeted intrusions should be present in plutons emplaced into pull-apart structures. Hanson and Glazner (1995) clarified this matter by calculating thermal models that show that if opening occurs at a rate of ~1 cm/yr or faster, then sheeted intrusions with chilled margins need not form at depths greater than 1 km or so.

The fault and vein patterns documented around the Grasberg Igneous Complex are compatible with the idea that a pull-apart process was fundamental in creating pathways for intrusion. Strike-slip movement along the 300° trend could have generated local left-stepping pull-apart openings along the 065°-trending tear faults that formed during shortening movements (Fig. 4). The field relationships indicate that the Grasberg Igneous Complex was emplaced into a major, ~2-km-wide pull-apart situated at a left-stepping offset connecting the Meren Valley and Ertsberg No. 1 faults. The connection was the Grasberg tear fault. The resultant pull-apart crosscuts the Yellow Valley syncline, one of the major folds in the district.

Field relationships are more obscure in other parts of the mining district because of cover and rugged topography, but map patterns allow us to infer that the major intrusions were similarly localized along other pull-apart pathways in the northwest-trending left-lateral strike-slip system. The Karume intrusion was emplaced into a dilated part of the southwest extension of the Carstenz Valley fault, and the Ertsberg intrusion was emplaced into the New Zealand Pass fault (Fig. 17). The southern boundary of the system is the Wanagon fault zone along which the Wanagon intrusion was emplaced into a bend. Two of the major fault zones along the HEAT Road strike northwest toward the Lembah Tembaga intrusion and southeast into the Ertsberg pluton. Lembah Tembaga formed as a plug into a small pull-apart zone. These fault trends—along with the dominance of minor normal faulting and veining indicating northwest-southeast extension along the HEAT Road—seemingly reflect larger movement patterns that could account for why the Ertsberg pluton is the largest in the district. The scattered occurrences of small dikes, sills, and plugs are explainable as offshoots from the main intrusion pathways.

The northwest-trending, left-lateral strike-slip, pull-apart system was active at 3 Ma, for this is the age of the Grasberg and Ertsberg intrusions. The time that regional shortening ended and strike-slip movements began is not directly constrained. It is inferred that strike-slip activity became active in the core of the highlands at ca. 4 Ma because this is the age of the oldest intrusion in the district.

Pull-apart zones in the strike-slip system would have a profound effect not just on localizing magma emplacement, but also on generating and localizing permeability for the escape of magmatic fluids that accumulated beneath cupolas at the top of stock/batholith magma chamber (Cloos, 2001). In the Grasberg pluton, the central pathway for intrusion and that for subsequent fluid flow and ore mineralization were the same. In the Ertsberg pluton, the magma spread near the surface, forming a laccolithic sill, and there were three distinct centers of mineralization. The Ertsberg, Gunung Bijih Timur Complex, and Dom ore skarns are obviously localized areas of magmatic fluid flow, and the fact that there are three separate mineralized areas suggests that

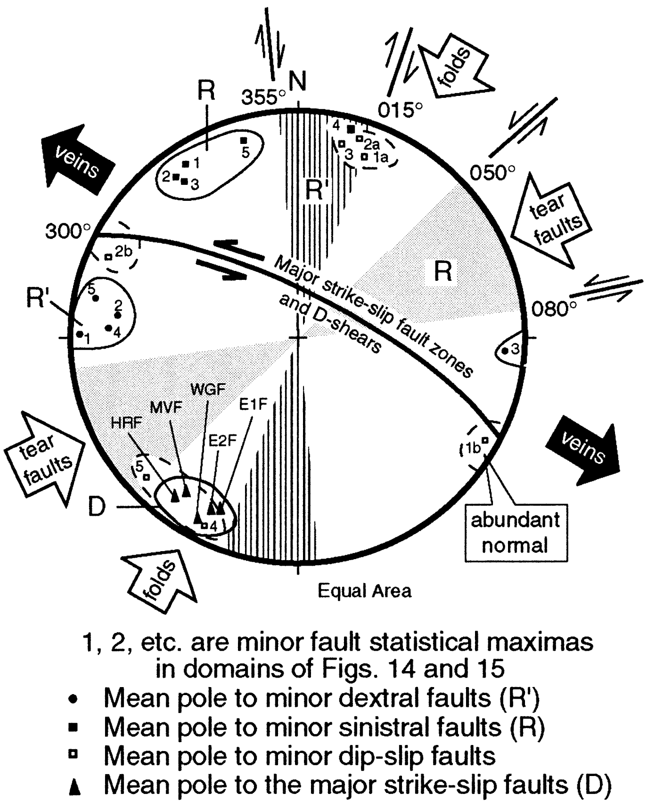

Figure 16. Lower-hemisphere equal-area stereogram summarizing relationships among all types of structural data. Large dark arrows represent the direction of extension as inferred from the veins. Large open arrows represent the principal axis of early shortening inferred from the kilometer-scale folding and the tear faulting. Triangles—mean poles to major fault zones; squares and dots—mean poles to minor faults. MVF—Meren Valley fault; E1F—Ertsberg No. 1 fault; HRF—HEAT Road fault; E2F—Ertsberg No. 2 fault; WGF—Wanagon fault.

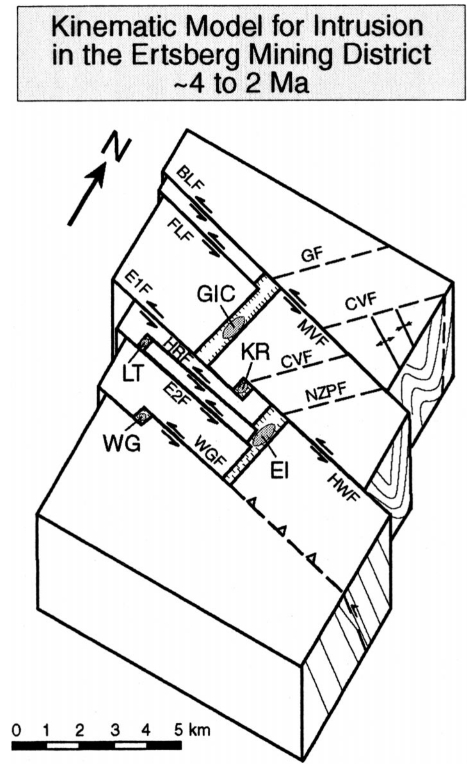

Figure 17. Schematic block diagram illustrating the proposed emplacement model for major intrusive bodies in the Ertsberg Mining District between 4 and 2 Ma. This kinematic model is based on geometric relationships of major left-lateral strike-slip fault zones, tear faults (dashed), and the location of major intrusive bodies. Intrusions: EI—Ertsberg intrusion; GIC—Grasberg Igneous Complex; KR—Karume intrusion; LT—Lembah Tembaga intrusion; WG—Wanagon intrusion. Strike-slip faults: MVF—Meren Valley fault; E1F—Ertsberg No. 1 fault; HRF—HEAT Road fault; E2F—Ertsberg No. 2 fault; WGF—Wanagon fault; BLF—Barat Laut fault; FLF—Fairy Lakes fault; HWF—Hanging Wall fault. Tear faults: GF—Grasberg fault; CVF—Carstensz Valley fault; NZPF—New Zealand Pass fault.

there may have been more than one feeder pathway for magma. Where magmas intrude and hydrothermal fluids flow, direct evidence of earlier faulting is largely, if not entirely, obliterated by recrystallization.

REGIONAL TECTONICS

Two distinct deformation events are recognized in the mining district: major shortening accommodated by kilometer-scale folding and minor reverse faulting, followed by hundreds of meters to perhaps 1 km or so of northwest-trending left-lateral strike-slip faulting concurrent with the magmatic activity and hydrothermal fluid flow (Fig. 17).

Stage 1 (ca. 12–4 Ma)

Prior to ca. 12 Ma, the folded rocks exposed in the mining district were on a stable passive margin where shallow-marine sedimentation continued to blanket the Australian continental basement. (Quarles van Ufford, 1996). Since ca. 12 Ma, kilometer-scale folds formed in the passive-margin strata as the northern edge of the Australian continent entered a northeast-dipping subduction zone beneath the Pacific plate. Convergence along an ~245° direction is indicated by the global plate-motion reconstructions of Scotese et al. (1988). Such motion would directly account for the ~065°-trending tear faults in the northeast part of the mining district (Fig. 4). As the folds became tight, subsidiary high-angle reverse faults formed (Wanagon fault, Ertsberg No. 2 fault, and Meren Valley fault).

In the simple kinematic picture deduced from the plate motions and the trend of the tear faulting, the expected orientation of folds should be close to 330°/150°. The 300°/120° trend is explainable as being due to (1) progressive rotation of growing en echelon folds during oblique convergence (i.e., deformation was thin-skinned) or (2) influence by basement structures on the orientation of folding in the sedimentary cover (thick-skinned deformation). Granath and Argakoesoemah (1989) concluded that major basement faults generated during Mesozoic rifting trend ~280° along the south flank of the western Central Range. Weiland and Cloos (1996) concluded that reversal of movement on one of these fault zones controlled the formation of the Mapenduma anticline, a giant (30-km-wide, 300-km-long) fold south of the mining district that is cored by basement rock. Fission-track thermochronology analysis indicates that this structure began to form at ca. 7 Ma, and its size indicates that shortening movements must have continued until 4 Ma or so.

Stage 2 (ca. 4–2 Ma)

The second stage of deformation in the mining district is comparatively minor, for it only involved hundreds of meters to 1 km or so of left-lateral strike-slip offset trend subparallel to the local ~300° grain of upturned bedding. Where crosscutting structures such as the northeast-trending tear faults generated during folding were present, left-stepping bends extended. At least four of the major strike-slip fault zones (Wanagon fault, Ertsberg No. 2 fault, Ertsberg No. 1 fault, Meren Valley fault) have breccias, igneous dikes, and mineralization indicating that the strike-slip faulting was a significant factor in creating pathways for intrusion and permeability for the flow of hydrothermal fluid.

The profound change in deformation style from regional folding to localized strike-slip offset is interpreted to be a manifestation of a short-lived change in the relative plate motion between the Australian and Pacific plates at ca. 4 Ma. We think that the strike-slip regime was the product of transform movement between the Australian plate and a broken off prong of the Pacific plate north of the island. This piece, the Caroline plate, had a short life as a distinct kinematic entity, from ca. 4 to 2 Ma (Fig. 3; Weissel and Anderson, 1978; Cloos, 1992).

The Bewani-Torricelli, Yapen, and Sorong fault systems along the north coast are left-lateral strike-slip zones with an overall trend of ~280° (Fig. 3). If these megastructures are ideal transform faults, the apparent Pacific-Australian motions during their formation had an azimuth of ~280°. This is very close to 270°, the optimal relative plate motion to activate strike-slip along the 300° trend of the upturned bedding. The timing of the change to major strike-slip faulting along northern New Guinea is well dated from the fact that the Bewani-Torricelli fault zone connects to the spreading centers in the Bismarck Sea. Magnetic anomalies indicate that these centers began to open at ca. 3.5 Ma (Taylor, 1979). Another nearby event related to the collision forming the island is the formation of the Woodlark spreading center as a propagating tear into the northeast corner of the Australian plate since ca. 3.5 Ma (Weissel et al., 1982). The western highlands are not currently the site of active faulting, on the basis of regional seismicity. In the Ertsberg district, glacial deposits, at least hundreds to probably several thousand years old, have been exposed by mining in many places. No fault offsets have ever been observed. We think the cessation of magmatic activity at ca. 2.5 Ma corresponds to the cessation of strike-slip faulting in this part of the highlands.

The concept advocated here is that strike-slip movements were distributed across the Central Range between ca. 4 Ma and ca. 2 Ma as part of reoriented movements (well-dated by the opening of the Bismarck and Woodlark spreading centers) associated with collisional orogenesis (see Cloos, 1993). The most important tectonic effect was the temporary formation of the Caroline plate as a distinct kinematic entity north of the island; this event caused a change from convergent to left-lateral transform motions. Since ca. 2 Ma, the broken corner became reattached to the Pacific plate, and Australian-Pacific relative motion has been mostly accommodated by slightly convergent transform motion along the northern margin of the island (see Fig. 3).

CONCLUSIONS

Structural analyses along an ~15-km-long transect of the HEAT and Grasberg Roads in the Ertsberg (Gunung Bijih) Mining District reveal several new facts concerning the internal deformation of the Central Range of Irian Jaya.

1. There were two distinct stages of deformation since ca. 12 Ma. The first stage generated a series of northwest-trending (π-axis = 300°) folds with associated tear and reverse faults. The second stage resulted in significant left-lateral, strike-slip faulting subparallel to the regional strike of upturned bedding.

2. Five major northwest-trending (~300°) strike-slip fault zones were found in the mining district that are nearly parallel to the upturned sedimentary bedding. They were the location of tens to hundreds of meters of left-lateral offset that cumulatively totaled ~1 km.

3. The pattern of minor strike-slip faulting in the domains between the major fault zones mimics the minor fault patterns found in the classic strike-slip clay-cake experiments of Riedel (1929) and Tchalenko (1970). Faults trending 040°–070° have left-lateral slickensides (rakes of 5°–15°) plunging to the northeast and are interpreted as R shears. Faults trending 355°–015° have right-lateral slickensides (rakes of 10°–20°) plunging to the north and are interpreted as R′ shears. D shears are subsidiary and trend ~280°–300°.

4. Calcite and pyrite vein orientations show consistent northwest-southeast direction of extension.

5. The change in deformation styles from shortening to strike-slip offset is explained as being due to a change in relative plate motion between the Pacific and Australian plates at ca. 4 Ma. From ca. 4–2 Ma, transform motion along an ~280° trend caused left-lateral strike-slip offset in the core of the Central Range. This deformation formed pathways for magma ascent and had a profound effect on localizing hydrothermal activity. Magma ascent in the mining district, most obviously for the Grasberg Igneous Complex, was localized in the center of a pull-apart zone.

ACKNOWLEDGMENTS

We thank J.R. Moffett and all of the geologists and staff of Freeport McMoRan, Inc. and P.T. Freeport Indonesia, whose support and work enabled students, faculty, and research scientists at the University of Texas, Austin, to study the geology of the Ertsberg Mining District in Irian Jaya (Papua), Indonesia. Over the years, the work of, and discussions with, Dave Potter, Steve van Nort, George MacDonald, Clark Arnold, Eddy Suwardy, Art Ona, Jay Pennington, Sugeng Widodo, Chuck Brannon, Wahyu Sunyoto, Al Edwards, Sanusi Sukarya, Ian Tasiran, Dave Mayes, Nurhamid, Kris Hefton, Keith Parris, Widodo Margotomo, Bambang Trisetyo, Larry Johnson, and Doug McKenzie contributed greatly to making this paper possible. Similarly, we thank our University of Texas colleagues Tim McMahon, Andrew Quarles van Ufford, Richard Weiland, Paul Warren, Sarah Penniston-Dorland, Eric Beam, Cori Lambert, Roy Luck, Fred McDowell, Todd Housh, Eric James, and Bob Boyer for discussions over the years. We also thank Sharon Mosher, Rich Kyle, Carl Jacobson, and Dave Wiltschko, who served on Sapiie's dissertation committee. Reviews by Basil Tikoff, James Granath, and Ken McCaffrey significantly improved the manuscript and are greatly appreciated. This research was supported by a grant from Freeport McMoRan, Inc. Ertsberg Project Contribution No. 20.

REFERENCES CITED

Abers, G., and McCaffrey, R., 1988, Active deformation in the New Guinea fold and thrust belt: Seismological evidence for strike-slip faulting and basement involved thrusting: Journal of Geophysical Research, v. 93, p. 13,322–13,354.

Cloos, M., 1992, Origin of the Caroline block and plate: Tectonic response to change in Pacific plate motion at ~43 and 4 Ma: Geological Society of America Abstracts with Programs, v. 24, no. 7, p. A185.

Cloos, M., 1993, Lithospheric buoyancy and collisional orogenesis: Subduction of oceanic plateaus, continental margins, island arcs, spreading ridges, and seamount: Geological Society of America Bulletin, v. 105, p. 715–737.

Cloos, M., 2001, Bubbling magma chambers, cupolas, and porphyry copper deposits: International Geology Review, v. 43, p. 285–311.

Cooper, P., and Taylor, B., 1987, Seismotectonics of New Guinea: A model for arc reversal following arc-continent collision: Tectonics, v. 6, p. 53–68.

Dewey, J.F., and Bird, J.M., 1970, Mountain belts and the new global tectonics: Journal of Geophysical Research, v. 75, p. 2625–2647.

Dow, D.B., and Sukamto, R., 1984a, Late Tertiary to Quaternary tectonics of Irian Jaya: Episodes, v. 7, p. 3–9.

Dow, D.B., and Sukamto, R., 1984b, Western Irian Jaya: The end-product of oblique plate convergence in the late Tertiary: Tectonophysics, v. 106, p. 109–139.

Dow, D.B., Robinson, G.P., Hartono, U., and Ratman, N., 1988, Geology of Irian Jaya: Indonesia, Irian Jaya Geological Mapping Project, in cooperation with the Australia Bureau of Mineral Resources, on behalf of the Indonesia Department of Mines and Energy and the Australian Development Assistance Bureau, 298 p.

Glazner, A.F., 1991, Plutonism, oblique subduction, and continental growth: An example from Mesozoic of California: Geology, v. 19, p. 784–786.

Granath, J.W., and Argakoesoemah, R.M.I., 1989, Variation in structural style along the eastern Central Range thrust belt: Proceedings of the Indonesian Petroleum Association, v. 18, p. 79–89.

Hamilton, W., 1979, Tectonics of the Indonesian region: U.S. Geological Survey Professional Paper 1078, 345 p.

Hanson, R.B., and Glazner, A.F., 1995, Thermal requirements for extensional emplacement of granitoids: Geology, v. 23, p. 213–216.

Hefton, K., and Kavalieris, I., compilers, 1997, COW-A preliminary geology map: P.T. Freeport Indonesia, scale 1:10,000, 1 sheet.

Housh, T., and McMahon, T.P., 2000, Ancient isotopic characteristics of Neogene potassic magmatism in western New Guinea (Irian Jaya, Indonesia): Lithos, v. 50, p. 217–239.

Hutton, D.H.W., 1982, A tectonic model for the emplacement of the Main Donegal Granite, NW Ireland: Geological Society [London] Journal, v. 139, p. 615–631.

Hutton, D.H.W., 1990, A new mechanism of granite emplacement: Intrusion in an active extensional shear zone: Nature, v. 343, p. 452–455.

Johnson, R.W., Mackenzie, D.E., and Smith, I.E.M., 1978, Delayed partial melting of subduction—modified mantle in Papua New Guinea: Tectonophysics, v. 46, p. 197–216.

Kamb, W.B., 1959, Ice petrofabric observations from Blue Glacier, Washington, in relation to theory and experiment: Journal of Geophysical Research, v. 64, p. 1891–1909.

Little, T.A., 1995, Brittle deformation adjacent to Awatere strike-slip fault in New Zealand: Faulting patterns, scaling relationships, and displacement partitioning: Geological Society of America Bulletin, v. 107, p. 1255–1271.

MacDonald, G.D., and Arnold, L.C., 1994, Geological and geochemical zoning of the Grasberg Igneous Complex, Irian Jaya, Indonesia: Journal of Geochemical Exploration, v. 50, p. 143–178.

Martodjojo, S., Sudradjat, D., Subandrio, E., and Lukman, A., 1975, The geology and stratigraphy along the road cut Tembagapura, Irian Jaya: Bandung, Indonesia, Institute of Technology, Bandung Report, 51 p. (unpublished).

McDowell, F.W., McMahon, T.P., Warren, P.Q., and Cloos, M., 1996, Pliocene Cu-Au–bearing igneous intrusions of the Gunung Bijih (Ertsberg) District, Irian Jaya, Indonesia: K-Ar geochronology: Journal of Geology, v. 104, p. 327–340.

McMahon, T.P., 1994a, Pliocene intrusions in the Ertsberg (Gunung Bijih) Mining District, Irian Jaya, Indonesia: Petrography, geochemistry, and tectonic setting [Ph.D. thesis]: Austin, University of Texas, 298 p.

McMahon, T.P., 1994b, Pliocene intrusions in the Gunung Bijih (Ertsberg) Mining District, Irian Jaya, Indonesia: Petrography and mineral chemistry: International Geology Review, v. 36, p. 820–849.

McMahon, T.P., 1994c, Pliocene intrusions in the Gunung Bijih (Ertsberg) Mining District, Irian Jaya, Indonesia: Major and trace element geochemistry: International Geology Review, v. 36, p. 925–946.

McMahon, T.P., 1999, The Ertsberg intrusion and the Grasberg Complex: Contrasting styles of magmatic evolution and Cu-Au mineralization in the Gunung Bijih (Ertsberg) Mining District, Irian Jaya, Indonesia: Jurusan Teknik Geologi–Institute Teknologi Bandung, Buletin Geologi, v. 31, no. 3, p. 123–132.

McMahon, T.P., 2000a, Magmatism in an arc-continent collision zone: An example from Irian Jaya (western New Guinea), Indonesia: Jurusan Teknik Geologi–Institute Teknologi Bandung, Buletin Geologi, v. 32, no. 1, p. 1–22.

McMahon, T.P., 2000b, Origin of syn- to post-collisional magmatism in New Guinea: Jurusan Teknik Geologi–Institute Teknologi Bandung, Buletin Geologi, v. 32, no. 2, p. 89–104.

Meinert, L.D., Hefton, K.H., Mayes, D., and Tasiran, I., 1997, Geology, zonation, and fluid evolution of the Big Gossan Cu-Au skarn deposit, Ertsberg District, Irian Jaya: Economic Geology, v. 92, p. 509–534.

Mertig, H.J., Rubin, J.N., and Kyle, J.R., 1994, Skarn Cu-Au orebodies of the Gunung Bijih (Ertsberg) District, Irian Jaya, Indonesia: Journal of Geochemical Exploration, v. 50, p. 179–202.

Milsom, J., 1985, New Guinea and the western Melanesian arcs, *in* Nairn, A.E.M., et al., eds., The ocean basins and margins: The Pacific Ocean, Volume 7A: New York, Plenum Press, p. 551–605.

Nash, C., Artmont, G., Gillan, M.L., Lennie, D., O'Connor, G., and Parris, K.R., 1993, Structure of the Irian Jaya mobile belt, Irian Jaya, Indonesia: Tectonics, v. 12, p. 519–535.

Parris, K., 1994, Preliminary geological data record, Timika, Irian Jaya: P.T. Freeport Indonesia, 1:250,000 sheet area, 38 p. (unpublished).

Paterson, S.R., and Fowler, T.K., Jr., 1993, Re-examining pluton emplacement processes: Journal of Structural Geology, v. 15, p. 191–206.

Pennington, J., and Kavalieris, I., 1997, New advances in the understanding of the Grasberg copper-gold porphyry system, Irian Jaya, Indonesia: Pacific treasure trove—Copper-gold deposits of the Pacific rim: Prospectors and Developers Association of Canada, Annual Convention and Trade Show, p. 79–97.

Petit, J.-P., 1987, Criteria for the sense of movement on fault surfaces in brittle rocks: Journal of Structural Geology, v. 9, p. 597–608.

Pieters, P.E., Pigram, C.J., Trail, D.S., Dow, D.S., Ratman, N., and Sukamto, R., 1983, The stratigraphy of Irian Jaya: Bandung, Indonesia, Geological Research and Development Centre Bulletin, no. 8, p. 14–48.

Pigram, C., and Panggabean, H., 1984, Rifting of the northern margin of the Australian continent and the origins of some microcontinents in eastern Indonesia: Tectonophysics, v. 107, p. 331–353.

Puntodewo, S.O., McCaffrey, R., Calais, E., Bock, Y., Rais, J., Subarya, C., Poewariardi, R., Stevens, C., Genrich, J., Fauzi, Zwick, P., and Wdowinski, S., 1994, GPS measurements of crustal deformation within the Pacific-Australia plate boundary zone in Irian Jaya, Indonesia: Tectonophysics, v. 237, p. 141–153.

Quarles van Ufford, A., 1996, Stratigraphy, structural geology, and tectonics of a young forearc-continent collision, western Central Range (western New Guinea), Indonesia [Ph.D. thesis]: Austin. University of Texas, 420 p.

Riedel, W., 1929, Zur mechanick geologischer brucherscheinungen: Zentralblatt für Mineralogie, Geologie un Palaeontologie, Abhandlungen B, p. 354–368.

Ripper, I.D., and McCue, K.F., 1983, The seismic zone of the Papuan fold belt: Australia Bureau of Mineral Resources Journal of Australian Geology and Geophysics, v. 8, p. 147–156.

Sapiie, B., 1998, Strike-slip faulting, breccia formation and porphyry Cu-Au mineralization in the Gunung Bijih (Ertsberg) Mining District, Irian Jaya, Indonesia [Ph.D. thesis]: Austin, University of Texas, 304 p., 4 plates.

Sapiie, B., Natawidjaya, D.H., and Cloos, M., 1999, Strike-slip tectonics of New Guinea: Transform motion between the Caroline and Australian plates, *in* Busono, I., and Alam, H., eds., Developments in Indonesian tectonics and structural geology: Indonesian Association of Geologists, 28th Annual Convention, Jakarta, Indonesia, 30 November–1 December 1999, Proceedings, v. 1, p. 1–15.

Scotese, C.R., Gahagan, L.M., and Larson, R.L., 1988, Plate tectonic reconstructions of the Cretaceous and Cenozoic ocean basins: Tectonophysics, v. 155, p. 27–48.

Sillitoe, R.H., 1973, The tops and bottoms of porphyry copper deposits: Economic Geology, v. 68, p. 799–815.

Taylor, B., 1979, Bismarck Sea: Evolution of back-arc basin: Geology, v. 7, p. 171–174.

Tchalenko, J.S., 1970, Similarities between shear zones of different magnitudes: Geological Society of America Bulletin, v. 81, p. 1625–1640.

Tikoff, B., and Teyssier, C., 1992, Crustal-scale, en echelon ''P-shear'' tensional bridges: A possible solution to the batholithic room problem: Geology, v. 20, p. 927–930.

Titley, S.R., 1981, Geologic and geotectonic setting of porphyry copper deposits in the Southern Cordillera: Arizona Geological Society Digest, v. 14, p. 79–9.

Twiss, R.J., and Moores, E.M., 1992, Structural geology: New York, W.H. Freeman and Company, p. 100–127.

van Nort, S.D., Atwood, G.W., Collinson, T.B., Flint, D.C., and Potter, D.R., 1991, Geology and mineralization of the Grasberg copper-gold deposit: Mining Engineering, v. 43, p. 300–303.

Visser, W.A., and Hermes, J.J., 1962, Geological results of the exploration for oil in the Netherlands New Guinea: Verhandelingen van het Koninklijk Nederlands Geologisch Mijnbouwkundig Genootschap, Geologische Serie, v. 20, 265 p.

Warren, P.Q., 1995, Petrology, structure and tectonics of the Ruffaer metamorphic belt, west central Irian Jaya, Indonesia [M.A. thesis]: Austin. University of Texas, 338 p.

Wegener, A., 1929, The origin of continents and oceans, J. Biram translation, 1966: New York, Dover, 231 p.

Weiland, R.J., 1999, Emplacement of the Irian ophiolite and unroofing of the Ruffaer metamorphic belt of Irian Jaya, Indonesia [Ph.D. thesis]: Austin, University of Texas, 526 p.

Weiland, R.J., and Cloos, M., 1996, Plio–Pleistocene asymmetric unroofing of the Irian fold belt, Irian Jaya, Indonesia: Apatite fission-track thermochronology: Geological Society of America Bulletin, v. 108, p. 1438–1449.

Weissel, J.K., and Anderson, R.N., 1978, Is there a Caroline plate?: Earth and Planetary Science Letters, v. 41, p. 143–158.

Weissel, J.K., Taylor, B., and Karner, G.D., 1982, The opening of the Woodlark Basin, subduction of the Woodlark spreading system, and the evolution of northern Melanesia since mid-Pliocene time: Tectonophysics, v. 87, p. 253–277.

Widodo, S., Manning, P., Wiwoho, N., Johnson, L., Belluz, N., Kusnanto, B., MacDonald, G., and Edwards, A., 1999, Progress in understanding and developing the Kucing Liar orebody, Irian Jaya, Indonesia, *in* Proceedings of the International Congress on Earth Science, Exploration and Mining Around the Pacific Rim (PacRim'99): Australasian Institute of Mining and Metallurgy Publication Series 4, p. 499–507.

Manuscript Received by the Society 7 June 2001
Revised Manuscript Received 27 January 2002
Manuscript Accepted 27 January 2003

Printed in the USA